Nuclear Engineering and Design 346 (2019) 140–156

Contents lists available at ScienceDirect

Nuclear Engineering and Design

journal homepage: www.elsevier.com/locate/nucengdes

Seismic capacity and fragility analysis of an ASR-affected nuclear containment vessel structure

Victor E. Saouma[a,b,*], Mohammad Amin Hariri-Ardebili[a,b]

[a] Department of Civil Environmental and Architectural Engineering, University of Colorado, Boulder, CO, USA
[b] X-Elastica LLC, Boulder, CO, USA

ARTICLE INFO

Keywords:
Nuclear containment vessel structures
Seismic analyses
Fragility curves
Alkali silica reaction

ABSTRACT

Alkali silica reaction (ASR) is a nefarious one that has been observed in many dams. Its recent discovery in a nuclear containment vessel structure (NCVS) in the U.S. has taken the industry by surprise, and has spurred much interest. Of particular concern is whether the degraded concrete will result in diminished resistance to seismic excitation of a NCVS.

This three parts paper will first contextualize fragility analysis within the general framework of the Seismic Probabilistic Risk Assessment (SPRA) described by the Nuclear Regulatory Commission (NRC). Also reviewed are the challenges confronting the nuclear industry in the twenty first century. The second part is an extensive literature survey on published work related to seismic analysis of NCVS. Finally, the third part will develop a detailed seismic analysis of a fictitious NCVS suffering from ASR. Starting with the theoretical underpinning and concluding with the structure capacity and fragility curves.

The study will show that ASR can reduce the structural capacity of a NCVS, and the impact will be much greater for high probability low intensity ground motions (such as the operating based one) than for the low probability high intensity ones.

1. Introduction

1.1. Motivation

This paper introduction is best accomplished by quoting ASCE 4-16 (2016).

> *Regulatory government agencies are frequently faced with decisions related to the seismic design of operating nuclear facilities…As new information becomes available, the design basis may be challenged. … Because of its pervasive nature, an earthquake will"seek out" facility vulnerabilities…At issue is whether the changes can be accommodated within the inherent capacity of the original design or whether facility modifications are required.… current design practice does not provide a picture of the actual margin to failure, nor does it provide enough information to make realistic estimates of seismic risk…The seismic probabilistic risk assessment (SPRA) is an integrated process that includes consideration of the uncertainty and randomness of the seismic hazard, structural response, and material capacity parameters to give a probabilistic assessment of risk.*

Until fairly recently, the only imaginable *new information* was increased ground motion records and results of internal or external stressors. Though potential concrete degradation (e.g. alkali silica reaction; ASR) in a nuclear containment vessel structure (NCVS) has long been recognized (Graves et al., 2013), there were no provisions to handle this situation. Hence, when ASR was found in an NCVS, industry and regulatory agencies entered into uncharted territory with (to the best of the authors' knowledge) practically no input from the research community.

Such is the motivation for this paper.

1.2. Role of Fragility Analyses within the Probabilistic Risk Assessment [1]

Whereas this manuscript focuses on the seismic capacity and fragility analysis, it is important to contextualize their role inside the broader scope of a seismic probabilistic risk assessment (SPRA) which is a well-established methodology within the nuclear industry.

Probabilistic risk (or safety) assessment (PRA) consists of an analysis of the operations of a particular nuclear power plant (NPP), which focuses on the failures or faults that can occur to components, systems or

* Corresponding author at: Department of Civil Environmental and Architectural Engineering, University of Colorado, Boulder, CO, USA.
E-mail address: saouma@colorado.edu (V.E. Saouma).

[1] This section is largely based on the input of an anonymous reviewer.

https://doi.org/10.1016/j.nucengdes.2019.02.011
Received 18 October 2018; Received in revised form 5 February 2019; Accepted 14 February 2019
Available online 14 March 2019
0029-5493/

structures, and that can lead to damage and ultimately to the release of radioactive material, especially the fission products and actinides within the reactor fuel (Beckjord et al., 1993). Hence, the analysis seeks to identify the initiating events and the sequence of possible events that can lead to various levels of damage.

The first attempt to categorize accidents levels was the seminal paper of Farmer (1967). Drawing on this early work, in 1972 the US Atomic Energy Commission initiated the first comprehensive assessment of the risks associated with nuclear power plants by examining the system design and operating practices at two specific plants and using composite models to represent site meteorology and population density. The results were published in WASH-1400 (1975). This document concluded that for plants analyzed, the risk of nuclear reactor accidents is much smaller than other man-made and natural events to which society is generally already exposed. Another important outcome of this document was an extension of the work of Farmer (1967) to structure NPP's PRAs in three levels. Level 1: models the risk of damage of the reactor cored (*severe accident*); Level 2: analyzes the progression of an accident by considering how the containment structures and systems respond to the accident, which varies based on the initial status of the structure or system and its ability to withstand the harsh accident environment; Finally, Level 3: PRA is the *consequence analysis* resulting from radioactive material released in a severe accident. Hence, the safety philosophy of NPP design is built around the concept of defense-in-depth, which includes the concept of multiple barriers (Ashar et al., 2001). The NCVS being the final barrier against the release of radioactive material to the environment.

The 1979 accident at Three Mile Island substantially changed the character of the analysis of severe accidents worldwide. Kemeny (1979) and Rogovin and Grampton (1980) (the major investigations of that accident) recommended that PRA be used to complement the traditional deterministic methods of analyzing NPP safety and that probabilistic safety goals be developed for nuclear plants. The first PRA studies were limited to the assessment of events initiated by internal plant faults but were later extended to include external event initiators such as seismic leading to an SPRA (NUREG 1150, 2018). In common practice today, the principal outputs of an SPRA are core damage frequency (CDF) and large early release frequency (LERF) (NUREG-2201, 2016). In general for regulatory purposes it is adequate to only calculate CDF and LERF and no detailed Level 3 are required.

ASME (RA-S, ASME, 2008) and EPRI (EPRI, 2003) have developed guidelines and training for the performance of SPRA that are used by virtually all utilities in the U.S. for the analysis of their plants. Furthermore, prior to the Fukushima accident, all U.S. NPPs were required to perform an analysis of the risk of external events, including seismic through an Individual Plant Examination for External Events (IPEEE) (IPEEE, 0000; EPRI, 2000). These assessments either used SPRA or a simplified-SPRA approaches.

It should be emphasized that an SPRA is not performed for the Operating Basis Earthquake (OBE) or Safe Shutdown Earthquake (SSE) ground motions but only for the very low probability high intensity ones (frequency on the order of 1×10^{-6} per year or lower).

Finally, after Fukushima, plants were required to reevaluate the potential impact of external events on their structures (EPRI, 2013) as in some cases the seismic stressor may have been underestimated (Hardy et al., 2015).

In response to severe unanticipated seismic loads: a) the NCVS may fail to perform its function in maintaining leak tightness (liner damage and concrete cracking); and b) an internal structure supporting vital equipment (such as pumps, valves, pipes, or electrical cabinets) could lead to severe fuel damage. It should be emphasized that should there be no severe fuel damage (Level 1 above), it does not matter whether or not the NCVS maintains its integrity. Thus, the principal risk measure, CDF, is unaffected by NCVS integrity.

Whereas an SPRA study should include: 1) seismic hazard analysis; 2) structure/equipment fragility assessment; 3) accident sequence analysis; and 4) consequence (risk) evaluation analogies with subsequently developed Performance Based Earthquake Engineering (PBEE) for buildings is highlighted in Appendix B. Mostly inspired by PBEE, this paper will focus on the first two ingredients of an SPRA.

1.3. Guidelines

The integrity of a NPP is ensured by many guidelines. All of them have been written for the design of new structures, and only those related to SPRA address the existing NPPs.

General design principles are enunciated in Asme (2015). ASCE/SEI 43-05 (2005) stipulates that the seismic demand and structural capacity evaluations should have enough conservatism to achieve less than 1% probability of unacceptable performance for the design base earthquake (DBE) and that than 10% probability of unacceptable performance for a ground motion equal to 150% of DBE. These demands will necessitate the elaboration of fragility curves. Analysis guidelines can be found in ASCE 4-16 (2016) where a "non-mandatory" evaluation beyond the design basis SPRA is suggested. A similar (but less explicit) set of guidelines is given by IAEA (2009).

1.4. Anatomy of a probabilistic seismic analysis

With reference to the outcome of an SPRA mentioned above, this study is limited to the first two components and four steps are defined and then used, Fig. 1:

Aleatory Uncertainties represent variability that cannot be reduced but can be characterized. In this study, it is associated with ground motion selection. This starts with the hazard curves, site identifications, deaggregation model, and site specific acceleration response spectra. Finally, a set of real ground motions are selected and scaled to be consistent in the aggregate with the design response spectrum (Lapajne and Fajfar, 1997; Jayaram et al., 2011; Dolšek, 2012; Bradley et al., 2017). Alternatively, one may generate synthetic ground motion or even intensifying acceleration functions (Mashayekhi et al., 2018; Rezaeian and Der Kiureghian, 2008).

Epistemic Uncertainties represent variability that can be reduced by data collection or experimentation. In this study, it is associated with material and modeling and is best accomplished through Monte Carlo Simulation (MCS) Family (Vamvatsikos and Fragiadakis, 2010; Hariri-Ardebili and Saouma, 2016). The finite element model preparation is included in this block.

Finite Element Simulations where the preceding two uncertainties are combined and dynamic analyses performed. Again, whereas response spectrum method (RSM) was adequate early on (Ashar et al., 2001), time history is now strongly recommended. The analyses should be nonlinear so as to capture the various levels of engineering demand parameters (EDP). Different techniques exist for multiple dynamic analyses (Vamvatsikos and Cornell, 2002; Jalayer, 2003; Jalayer et al., 2015; Zentner et al., 2011; Huang et al., 2017).

Post-Processing of the results to extract EDPs, construct capacity functions (Hariri-Ardebili and Saouma, 2017), and finally compare the results with multiple limit states (LS) functions and drive fragility curves or surfaces Baker (2015), Porter (2017), Huang et al. (2011), Huang et al. (2011). Finally, it should be noted that not all SPRA encompass the epistemic uncertainties, and few of them perform a nonlinear time history analysis.

1.5. Challenges

In the spirit of ASCE 4-16 (2016), the nuclear industry is confronted with mounting challenges to the design basis of existing NCVS:

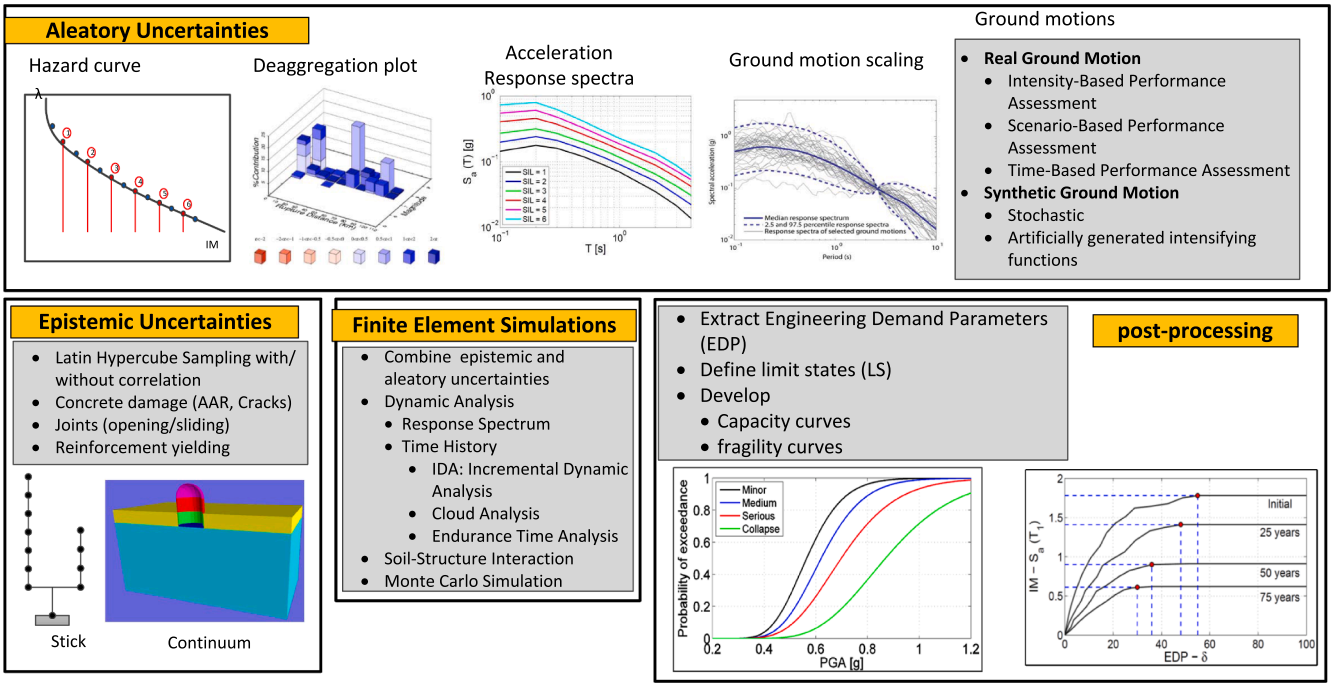

Fig. 1. Anatomy of a seismic probability risk assessment.

Beyond Design Basis Loads Though severe accident management guidelines have long been in place prior to the Fukushima accident, the Tohoku earthquake[2] highlighted the fact that for some operating nuclear power plants, available seismic data and models show increased seismic hazard estimates (Miller et al., 2011). As a result, orders were issued by the NRC to develop mitigation strategies for beyond design-basis external events (ADAMS Accession No, 2012).

Accidental and unanticipated damage. A perfect example is the delamination (or splitting crack along post-tensioning sleeves) resulting from the cable de-tensioning of Crystal-River 3 (Progress Energy, 2009). The reactor was ultimately decommissioned for financial reasons.

ASR Induced Ageing which has already affected an NCVS. Accordingly, the NRC has issued notices alerting NPP operators of this potential problem (ML112241029, 2011).

Second License Renewal Beyond 60 Years As of February 2018, the NRC has renewed the operating licenses of 89 commercial nuclear reactors through the process described in NRC (2015) (from 40 to 60 years). The NRC and the industry are currently focusing on "subsequent license renewals" which would authorize plants to operate up to 80 years. The NRC has developed guidance for staff and licensees specifically for the subsequent renewal period. The first subsequent license renewal application, for the Turkey Point Units 3 and 4 reactors, was submitted to the NRC in January 2018 (NRC Office of Public Affairs, 2018). In anticipation for this requirement a joint NRC-DOE (Department of Energy) effort objectively ranked the safety significance of materials degradation issues, particularly as they relate to subsequent license renewal. Using a Phenomena Identification and Ranking Table (PIRT), ASR, acid attack and creep emerged as secondarily important mechanisms (following impact of irradiation) (Graves et al., 2013).

Design Safety Issues May be a major challenge as one may be applying modern safety issues (i.e. accounting for increased regional seismicity or concrete deterioration) not fully grasped at the time of the design.

These challenges beg for modern solutions suitable for the structural safety assessment to generate fragility curves. At best, this will require at a dynamic analysis. This can be carried out through anyone of the following methods: a) static equivalent load; b) static pushover (linear or nonlinear, monotonic or cyclic); c) RSM; and d) time history: linear or nonlinear.

Historically, engineers have favored RSM as it was not CPU intensive. However, one must recognize that the RSM is a very approximate method which only produces positive values of displacements and member forces which are not in equilibrium; thus demand/capacity ratios have very large errors. Interestingly, Prof. Wilson is reported to have said:

> *Ray Clough and I regret we created the approximate response spectrum method for seismic analysis of structures in 1962…. At that time many members of the profession were using the sum of the absolute values of the modal values to estimate the maximum member forces. Ray suggested we use the SRSS method to combine the modal values. However, I am the one who put the approximate method in many dynamic analysis programs which allowed engineers to produce meaningless positive numbers of little or no value…After working with the RSM for over 50 years, I recommend it not be used for seismic analysis.* (Wilson, 2014).

In the context of design, demand in seismic assessment has traditionally been determined through an RSA and results linearly superimposed to those obtained from a static analysis with factored loads. Capacity in turn is assessed element by element in accordance with the provisions of ACI 318-14 (2014), Fig. 2(a). The dichotomy of a linear elastic analysis and a plastic design should be noted as it may cause the violation of the consistency condition of plasticity. Finally, some convoluted (heuristic and approximate) adjustments are made for the stress redistribution caused by cracking. The true structural safety factor remains unknown, even more so when localized concrete damage impact has not been properly accounted for.

Contrarily to the previous approach, a fragility analysis assesses the entire structure through multiple nonlinear transient analyses that will track the response throughout its load history. Ultimately probability of localized failure will be quantified. In some types of analysis, the full capacity curve of the structure (as opposed to element in the preceding

[2] It should be emphasized that despite its magnitude M_w = 9.0–9.1, the earthquake did not directly cause substantial damage. Failure was caused by the ensuing tsunami.

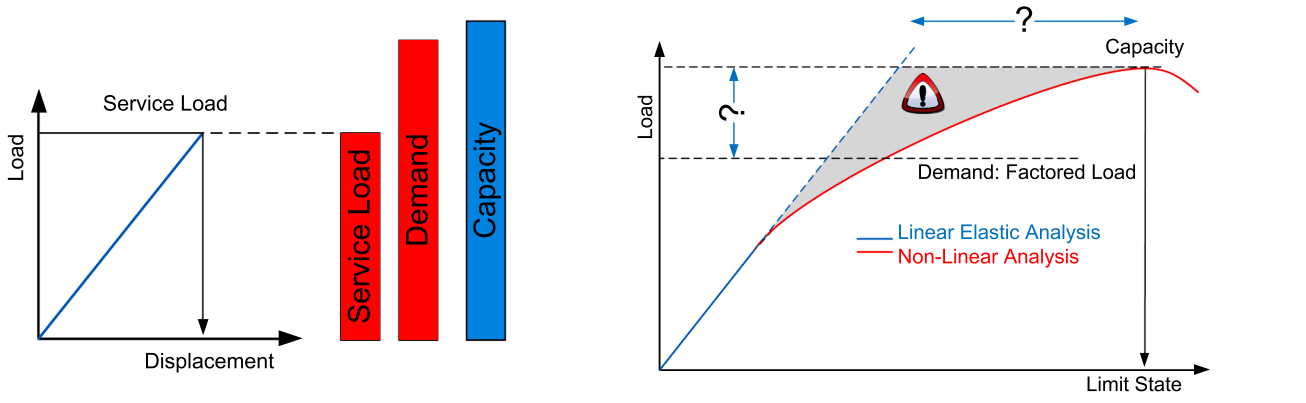

(a) Safety assessment of one elment

(b) Fragility Analysis of a structure

Fig. 2. Concerns with nonlinear analysis.

approach) can be determined if needed, Fig. 2(b).

Strength is not the only criteria, so-called serviceability (unfactored or service loads) is equally if not more important for NCVS. In this context, this will govern the formation of concrete cracks that may constitute a pathway for radioactive gas (in case of core damage, and liner failure). However, cracks can not be estimated from a linear elastic RSM-based analysis (neither the corresponding displacements), but can only be captured from a nonlinear analysis where the large inelastic displacements can be indeed captured.

Hessheimer and Dameron (2006) provided an excellent set of guidelines for the nonlinear analysis of NCVS; however, it seems to have been seldom consulted by published documents, and is by now mostly obsolete. More recently a short EPRI report (EPRI, 2017) addressed concrete degradation, beyond-design basis analysis, forensic analysis of concrete structures, and structural modeling. A comprehensive set of guidelines were submitted to the NRC by the authors (Saouma, 2017b).

2. Literature review

To place this study in context, it is important that the literature be properly reviewed. Hence this section will first address the seismic assessment of NCVS in terms of seismic hazard analysis, numerical simulations, and probabilistic risk assessment. Then, the analyses of concrete structures (NCVS in particular) affected by ASR will be reviewed. Review will be limited to peer-reviewed journal articles.

2.1. Seismic assessment of NCVS

2.1.1. Seismic hazard analysis

A seismic risk analysis has to start with a crisp identification of the site seismic hazard parameters (Verma et al., 2015). For nuclear sites, many analyses have been reported in the literature in terms of both deterministic and probabilistic seismic hazard analyses (PSHA). Ares and Fatehi (2013) provided an excellent introduction to the problematic of seismic hazard analysis.

Lapajne and Fajfar (1997) performed seismic hazard assessment for an existing NCVS in Slovenia that included multiple models to handle uncertainties in the data. Desai and Choudhury (2015) performed PSHA, one-dimensional equivalent linear ground response analysis, and developed the design uniform hazard response spectra (UHRS) of critical sites in Mumbai, India. Mohanty and Verma (2013) implemented a similar research on Kakrapar NCVS in western India. Choi et al. (2003) developed a probability-based scenario earthquakes for the Korean NCVS site using PSHA data. The response spectra were further modified by a factor correction to incorporate the near-fault earthquake effects. Similar study was performed by Nakajima et al. (2007). Klügel (2005) addressed the large scale PSHA of a Swiss NCVS and the corresponding potential overestimation of the seismic hazard in low seismic activity zones due to the inherent possibilities of unconstrained accumulation of uncertainties. Similar research was reported by Renault (2014).

2.1.2. Numerical simulations

Broadly speaking, there are two models for the FE analysis of NCVS: a) simplified LMSM approach; and b) detailed continuum model (using either solid or shell elements). The latter may include structural components (Frano et al., 2010; Nour et al., 2016; Sextos et al., 2017) and non-structural ones (i.e. reactor vessel and steam generator). However, it is a CPU intensive endeavor, specially in the nonlinear regime (Nakamura et al., 2010). The former is a much simplified one that consists of several lumped masses which form a column or tree as a numerical equivalent substitute to the actual structure (Nakajima et al., 2007; Lee et al., 2015; Park et al., 2017).

Modeling of foundation was addressed by Xu et al. (2005) who performed FE simulation of deeply embedded and/or buried NCVS structures. Simplified *vs* detailed soil-structure interaction (SSI) was investigated, and the seismic-induced earth pressures on the buried structures was quantified. Nakamura (2008) performed seismic response analyses of a nuclear reactor building deeply embedded in inhomogeneous soil considering frequency-dependent soil impedance in the time domain. Coleman et al. (2016) developed a nonlinear SSI model for NCVS which could be easily implemented in time-domain numerical codes. Kumar et al. (2015) investigated the seismic response of a NCVS modeled with both nonlinear Winkler springs, dashpots and gap elements in the context of bi-directional ground motions. Kabanda et al. (2015) performed a nonlinear time domain analysis focusing on the SSI in a nuclear power facility by first comparing the response through time and (simpler) frequency domains. They determined that the equivalent-linear frequency domain analysis amplifies some frequencies and results in higher structural acceleration than the nonlinear time domain analysis method which should be the preferred method. Ryu et al. (2010) proposed a 3D radial-shaped dynamic infinite elements fully coupled to finite elements for SSI analysis of NCVS system in a horizontally layered medium. Nakamura et al. (2012) studied the impact the irregular ground shape and adjacent buildings on the 3D nonlinear seismic response of NCVS buildings and highlighted its influence.

Joint elements to model the soil structure interface was investigated by Saxena et al. (2011). Base-isolation for NCVS has been numerically explored by various researchers (Ebisawa et al., 2000; Huang et al., 2010; Huang et al., 2013; Zhao and Chen, 2013; Perotti et al., 2013; Chen et al., 2014; Kumar et al., 2017; Kumar et al., 2017). In particular,

Medel-Vera and Ji (2016) performed an extensive comparative study of various seismic protection systems. Multiple adjacent NCVS require special attention. This potential interaction was studied by (Hakata, 2004; Hakata, 2007; Le Duy et al., 2016; Schroer and Modarres, 2013).

2.1.3. Probabilistic risk evaluation

There has been a gradual shift toward probabilistic risk evaluations in recent years. Kennedy and Ravindra (1984) were the first to introduce the concept of seismic fragility for NCVS. Fragility curves are conditional failure frequency curves plotted against peak ground acceleration (PGA). This general framework accounted for both aleatory and epistemic uncertainties. This first study was based on available data combined with judicious extrapolation of design information from plant structures and equipment. Medel-Vera and Ji (2016) proposed a very comprehensive framework for seismic probabilistic risk analysis of NCVS based on simulated accelerograms. This method neither used ground motion prediction equations nor Monte Carlo simulation (MCS). However, it demands longer use of computer resources as it is based on large number of nonlinear dynamic analyses. Huang et al. (2011), Huang et al. (2011) proposed a new procedure for probabilistic seismic risk assessment of NCVS using elements adopted from performance-based earthquake engineering of buildings. Seismic fragility of both structural and non-structural components were studied using nonlinear response history analysis combined with MCS. Zentner et al. (2011) presented the application of probabilistic analyses on a NCVS component based on MCS and fragility curves. They also discussed methods for statistical estimation of fragility curves.

Choi et al. (2008) performed nonlinear LMSM seismic simulation of a CANDU containment structure subjected to 30 near-fault earthquakes. Fragility analyses were performed for both linear and nonlinear analyses. Hoseyni et al. (2014) developed seismic fragility curves for a typical containment structure considering the SSI effect.

Aging and time-dependent response was first introduced by Ellingwood (1998) within a probabilistic framework. Age-related degradation of structures and passive components critical to the safe operation of NCVS was investigated by Braverman et al. (2004) through the development of fragility curves. Guimarães et al. (2006) further proposed the application of an adaptive neural fuzzy inference system to determine the fragility curves in degraded NCVS passive components. Huang et al. (2017) investigated the long-term performance (caused by shrinkage, creep, and relaxation of pre-stressing tendons) of a typical NCVS structure using a nonlinear FE model.

Sensitivities and uncertainties of FE model were quantified by Baušys et al. (2008). Response surfaces was used by De Grandis et al. (2009) in determining seismic fragility functions for equipment components in NCVS. System fragility, determined through combination of component ones accounting for both aleatory and epistemic uncertainties, was performed by Kim et al. (2011).

2.2. ASR analysis on concrete structures

Although there are many papers related to the experimental material and structural assessment of ASR-affected structures, few of them directly address numerical analyses. Majority of them addresses concrete dams (Léger et al., 1996; Saouma et al., 2007; Comi et al., 2009; Sellier et al., 2009; Pan et al., 2014; Lamea and Mirzabozorg, 2016). Few others address the impact of ASR on NCVS, i.e. Takatura et al. (2005) in Japan and Chénier et al. (2012) in Canada. Structural response of the bridge structures are reported in Li and Coussy (2002), Omikrine et al. (2016), Wojslaw and Wisniewski (2014), Hariri-Ardebili et al. (2018), while seismic response of a massive reinforced concrete structure is addressed by Saouma (2014).

For dams, Pan et al. (2012) have shown that ASR will indeed reduce their seismic load carrying capacity.

Probabilistic and statistical based analyses are becoming increasingly necessary in light of the uncertainties associated with ASR characteristics (Saouma et al., 2016; Hariri-Ardebili et al., 2018; Hariri-Ardebili and Saouma, 2018).

3. Case study

3.1. Motivation and contributions

Following the extensive literature review, attention is now focused on a specific case study. It is argued that whereas ASR *per se* may not seriously jeopardize the structural integrity of a NCVS under vertical service loads, this may not be the case under strong lateral (seismic) loads. Indeed many NCVSs have limited shear reinforcements. The major steps can be summarized as:

1. Prepare a detailed nonlinear finite element model including rock-containment interaction, concrete material nonlinearity, and interface joint around the NCVS.
2. Apply a pre-defined ASR expansion to the NCVS.
3. Develop two types of seismic excitations:
   - Scenario-based stochastic ground motions
   - Endurance time intensifying acceleration functions.
4. Determine the local and global failure modes.
5. Perform a set of nonlinear transient analyses using cloud computing and data mine the results.
6. Develop appropriate capacity and fragility curves for sound and ASR-affected NCVS.

For the first time, the integration of multiple state-of-the-art models is achieved to perform a key component of an SPRA for an NCVS with concrete deterioration.

3.2. Theoretical underpinnings of adopted model

Following the critical assessment of reported studies (state of the practice), and arguing that the subsequent case study will be based on the recommendations drawn from the state of the art approach above, the models used in this study are next discussed.

3.2.1. ASR constitutive model

The theoretical underpinning of the ASR model used in this paper has been presented by the authors separately (Saouma and Perotti, 2006; Saouma, 2014). The ASR expansion is considered to be a volumetric one:

$$\dot{\varepsilon}_V^{ASR}(t,\theta,RH) = \Gamma_t(f_t'|w_c,\ \sigma_I|\mathrm{COD}_{max}) \times \Gamma_c(\bar{\sigma},f_c') \times g(RH) \times \dot{\xi}(t,\theta) \times \varepsilon^{\infty}|_{\theta=\theta_0} \tag{1}$$

where ε^{∞} is the final volumetric expansion as determined from laboratory tests at temperature θ_0. $0 \leqslant \Gamma_t \leqslant 1$ is a parameter which reduces the expansion in the presence of large tensile stresses (macrocracks absorbing the gel), f_t' the tensile strength, and σ_I the major (tensile) principal stress. Similarly, $0 \leqslant \Gamma_c \leqslant 1$ is a parameter which accounts for the absorption of the gel due to compressive induced stresses, $\bar{\sigma}$ and f_c' are the hydrostatic stress, and the compressive strength of the concrete, respectively. $0 \leqslant g(RH) \leqslant 1$ is a function of the relative humidity (set to zero if the humidity is below 80%), $\dot{\xi}(t,\theta)$ the kinetics law given by (Larive, 1998)

$$\xi(t,\theta) = \frac{1-\exp\left(-\frac{t}{\tau_c(\theta)}\right)}{1+\exp\left(-\frac{(t-\tau_l(\theta))}{\tau_c(\theta)}\right)} \tag{2}$$

where τ_l and τ_c are the latency and characteristic times, respectively. The former corresponds to the inflexion point, and the latter is defined in terms of the intersection of the tangent at τ_l with the asymptotic unit value of ξ, Fig. 3(a). They are given by

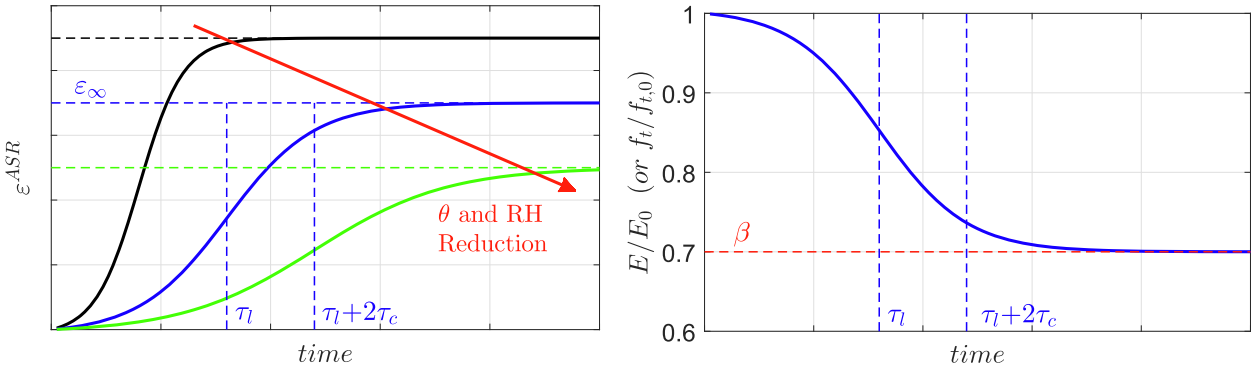

(a) Effect of temperature and RH (b) Degradation of E and f_t

Fig. 3. Main characteristics of the proposed ASR model.

$$\tau_l(\theta) = \tau_l(\theta_0)\exp\left[U_l\left(\frac{1}{\theta}-\frac{1}{\theta_0}\right)\right], \quad \tau_c(\theta) = \tau_c(\theta_0)\exp\left[U_c\left(\frac{1}{\theta}-\frac{1}{\theta_0}\right)\right] \tag{3}$$

expressed in terms of the absolute temperature ($\theta^oK = 273 + T^oC$) and the corresponding activation energies. U_l and U_c are the activation energies, minimum energy required to trigger the reaction for the latency and characteristic times, respectively. Once the volumetric ASR strain is determined, it is decomposed into a tensorial strain in accordance to the three weight factors associated with the principal stresses. Finally, degradation of the tensile strength and elastic modulus is accounted for as follows, Fig. 3(b):

$$\frac{E(t,\theta)}{E_0} = 1-(1-\beta_E)\times\xi(t,\theta), \quad \frac{f_t(t,\theta)}{f_{t,0}} = 1-(1-\beta_{f_t})\times\xi(t,\theta) \tag{4}$$

The model has been implemented by many (Pian et al., 2012; El Mohandes and Vecchiol, 2013; Rodriguez et al., 2011; Pan et al., 2013; Huang and Spencer, 2016; Huang et al., 2015; Ben-Ftima et al., 2016). The effect of temperature and relative humidity on the kinetics of the reaction is illustrated by Fig. 3(a) where the decrease in RH, results in a decrease of peak ASR while a lower temperature will slow the reaction. The anisotropic expansion model was recently validated by Liaudat et al. (2018) and the finite element code has been validated through a battery of problems in Saouma and Hariri-Ardebili (2016).

3.2.2. Dynamic excitation

Two approaches are pursued in this study. The first is based on endurance time analysis (ETA), and the second on a stochastic ground motion generation model.

3.2.3. Endurance time analysis

ETA is a dynamic pushover procedure which is used to estimate the seismic performance of structures when subjected to pre-designed intensifying excitation called Endurance Time Acceleration Function (ETAF) (Estekanchi et al., 2007). These simulated acceleration functions shake the structure from a low excitation level – with a structural response in the elastic range – to a high excitation level which causes failure. This full spectrum of response ranges is experienced during a single dynamic analysis, and thus, the structural performance is assessed on the basis of the time that it can sustain the imposed artificial excitation before a failure (yet to be defined).

The algorithm for an ETAF generation is fully described by Hariri-Ardebili et al. (2014). Fig. 4(a) shows the acceleration time history of a sample ETAF including the linear envelope, whereas the acceleration response spectra at different times are shown in Fig. 4(b). At any given time, the acceleration response spectrum of the ETAF remains proportional to the target. The following (semi-) linear correlation can be established between time and PGA or spectral acceleration (Hariri-Ardebili et al., 2016):

$$\mathrm{PGA}(t) = \frac{t}{t_{\mathrm{trg}}}\mathrm{PGA}^{\mathrm{trg}}, \quad S_a(T,t) = \frac{t}{t_{\mathrm{trg}}}S_a^{\mathrm{trg}}(T) \tag{5}$$

where the subscript trg refers to a known or target value.

The raw data from ETA can be further post-processed and presented in the form of so-called ETA function (maximum absolute values of EDP during the time interval from 0 to t):

$$\Omega(\mathrm{QoI}(t)) \equiv \max\{\mathrm{Abs}(\mathrm{QoI}(\tau)\colon \tau\in[0,t])\} \tag{6}$$

where QoI refers to quantity of interest (or engineering demand parameter, EDP).

ETA function can be converted to capacity function easily following two simple steps: 1) convert "time" to IM using Eq. 5, 2) invert the QoI-IM coordinate to IM-QoI. Finally, ETA functions are constructed based on a stochastic process, so at least three of them are required to reduce the statistical variation.

Stochastic Ground Motion Model There are two general classes of strong ground motion simulation techniques: physics-based and stochastic models. The former simulates ground motions by modeling the fault rupture, the resulting wave propagation, and the near-surface site amplification and is computationally expensive. The latter is empirical and directly simulate the ground motion. It is computationally inexpensive, and is equally applicable for high and low frequency motions (Yamamoto and Baker, 2013).

In this paper, the stochastic model proposed by Rezaeian and Der Kiureghian (2008), Rezaeian and Der Kiureghian (2010) is adopted. It is a fully non-stationary stochastic ground motion model based on a modulated filtered white-noise process including time-varying parameters. The temporal and spectral non-stationary characteristics are completely decoupled and this facilitates the identification of the model parameters. In addition, the limited number of parameters have physical interpretations.

In the continuous form, the model is formulated as:

$$x(t) = q(t,\boldsymbol{\alpha})\left\{\frac{1}{\sigma_h(t)}\int_{-\infty}^{t} h[t-\tau,\boldsymbol{\lambda}(\tau)]w(\tau)d\tau\right\} \tag{7}$$

where $x(t)$ is the ground acceleration, $q(t,\boldsymbol{\alpha})$ is a deterministic time-modulating function with parameters $\boldsymbol{\alpha}$ controlling the shape and intensity, $w(\tau)$ is a white-noise process and its integral presents a filtered white-noise process, and $\sigma_h^2(t)$ is the variance of the integral process. Since the right hand side expression is normalized by $\sigma_h(t)$, thus $q(t,\boldsymbol{\alpha})$ presents the standard deviation of $x(t)$.

- The modulating function has three parameters, $\boldsymbol{\alpha} = (I_A, D_{5-95}, t_{mid})$ which represent the Arias intensity, the effective duration, and the time at the middle of the strong-shaking phase.

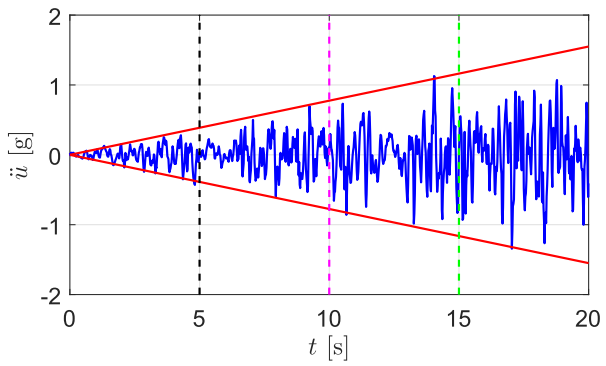

(a) Acceleration time history and the envelope

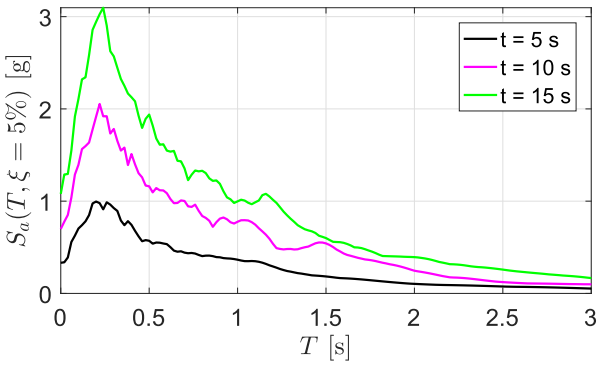

(b) Acceleration response spectra at different times

Fig. 4. Characteristics of a sample ETAF.

- The selected filter also has three parameters, $\lambda = (w_{mid}, w', \zeta)$ which represent the filter frequency at time t_{mid}, the rate of change of the frequency with time, and the damping ratio of the filter. These parameters control the predominant frequency and bandwidth of the signal process.

The ground motion model parameter vector can be summarized as $\{I_A, D_{5-95}, t_{mid}, w_{mid}, w', \zeta\}$. The predictive relationships are developed by fitting the stochastic model to a subset of the next generation attenuation relationships strong motion database. These predictive models are connected with the following earthquake and site characteristics: 1) moment magnitude (M_w); 2) distance to rupture (R_{rup}) in [km]; 3) shear wave velocity 30 m under the surface (V_{S30}) in [m/s]; and 4) fault mechanism (F_{mech}) either srtike-slip or reverse. The empirical equations have the following generic form:

$$\Phi^{-1}[F_\theta(\theta)] = \mu(M_w, R_{rup}, V_{S30}, F_{mech}; \boldsymbol{\beta}) + \eta + \sigma \tag{8}$$

where θ represents one of the six model parameters, $\Phi[.]$ is the standard Gaussian cumulative distribution function (CDF) and F_θ is the CDF of θ. μ is the predicted mean as a function of the earthquake and site characteristics and $\boldsymbol{\beta}$ represents the vector of regression coefficients. Furthermore, η and σ are normally distributed zero-mean random variables and refer to the inter-event and the intra-event errors, respectively. The regression coefficients, the variances of the error terms, and the correlations between the model parameters can be found in Rezaeian and Der Kiureghian (2008), Rezaeian and Der Kiureghian (2010).

3.2.4. Fragility analysis

The fundamentals of seismic fragility analysis have best been formulated by Kennedy and Ravindra (1984) and then refined by Porter et al. (2007) and Baker (2015). Amongst the three general numerical methods to generate fragility curves (Hariri-Ardebili et al., 2016) the so-called cloud method is adopted as it may be most suitable for the quantification of intermediary limit state (LS) functions (Jalayer et al., 2015; Mackie and Stojadinovic, 2005). Cloud-based fragility function for conditional seismic demand with a log-normal distribution (Cornell et al., 2002) can be expressed as:

$$\mathbb{P}[\text{QoI} \geqslant qoi|\text{IM}] = 1 - \Phi\left(\frac{\ln(qoi) - \ln(\eta_{\text{QoI|IM}})}{\beta_{\text{QoI|IM}}}\right) \tag{9}$$

where $\Phi(.)$ is the standard normal CDF, $\eta_{\text{QoI|IM}}$ is the median value of QoI given IM and $\beta_{\text{QoI|IM}}$ the logarithmic standard deviation and can be estimated as

$$\beta_{\text{QoI|IM}} \cong \sqrt{\frac{\sum(\ln(qoi_i) - \ln(a.\ \text{IM}^b))^2}{n-2}} \tag{10}$$

where n is the number of transient analyses, and a and b are regression parameters from $\eta = a.\ \text{IM}^b$.

3.2.5. Some considerations for seismic analyses

Of particular concerns in a dynamic analysis, specially when mass is assigned to the foundation, are: a) potential rocking that may cause uplift of the foundation or the NCVS itself; b) radiation damping; c) free field modeling; and d) necessity to assign the proper boundary conditions to the model.

Rocking of the NCVS itself, Fig. 5(a), is addressed by inserting zero thickness joint elements around the NCVS to mitigate it. Rocking of the foundation, Fig. 5(b), necessitates a two step analysis. First a static analysis (dead load and ASR) is performed with adequate vertical support, Fig. 5(c), to be followed by a dynamic one. The dynamic analysis is a restart with the initial state variables (stains/stresses) and the supports removed and replaced by nodal equivalent forces, Fig. 5(d). Furthermore, the dynamic analysis has the radiation damping achieved through properly tuned dashpots (Lysmer and Kuhlemeyer, 1969). The absence of vertical support will prevent the effect of "hammering" on the foundation by the inertial forces. Free field is not modeled in this investigation as it increase computational effort substantially, (Saouma et al., 2011).

3.3. Case study

3.3.1. Finite element mesh description

In light of recent evidence that ASR can reduce the shear strength by up to 20% (Saouma, 2017a), the impact of such a loss on the structural capacity of a NCVS excited by earthquakes is next ascertained through a state of the art driven analysis of a generic NCVS with dimensions inspired from NUREG/CR-6706 (2001). The structure will be first subjected to 40 years of ASR expansion followed by multiple seismic excitations (with or without ASR induced damage), and results will be compared with the response of the NCVS subjected to the same seismic excitations but without prior ASR expansion (Fig. 6B, C, and A respectively).

Outline of the analysis procedure is partially shown in Fig. 1 where after identification of the physical model site characteristics, probabilistic seismic hazard analysis and seismic hazard de-aggregation are performed. Then, ASR properties are identified, and dynamic excitations are generated through: a) ETAF, and b) scenario-based stochastic ground motions. Then, the FE analysis is performed in the cloud (i.e. using multiple CPU's) and finally capacity and fragility curves are derived for ETA and stochastic models, respectively. In each case, three analyses were performed, Fig. 6.

The selected and partially buried NCVS is schematically shown in Fig. 7(a). Note that only the concrete underneath the soil level will be

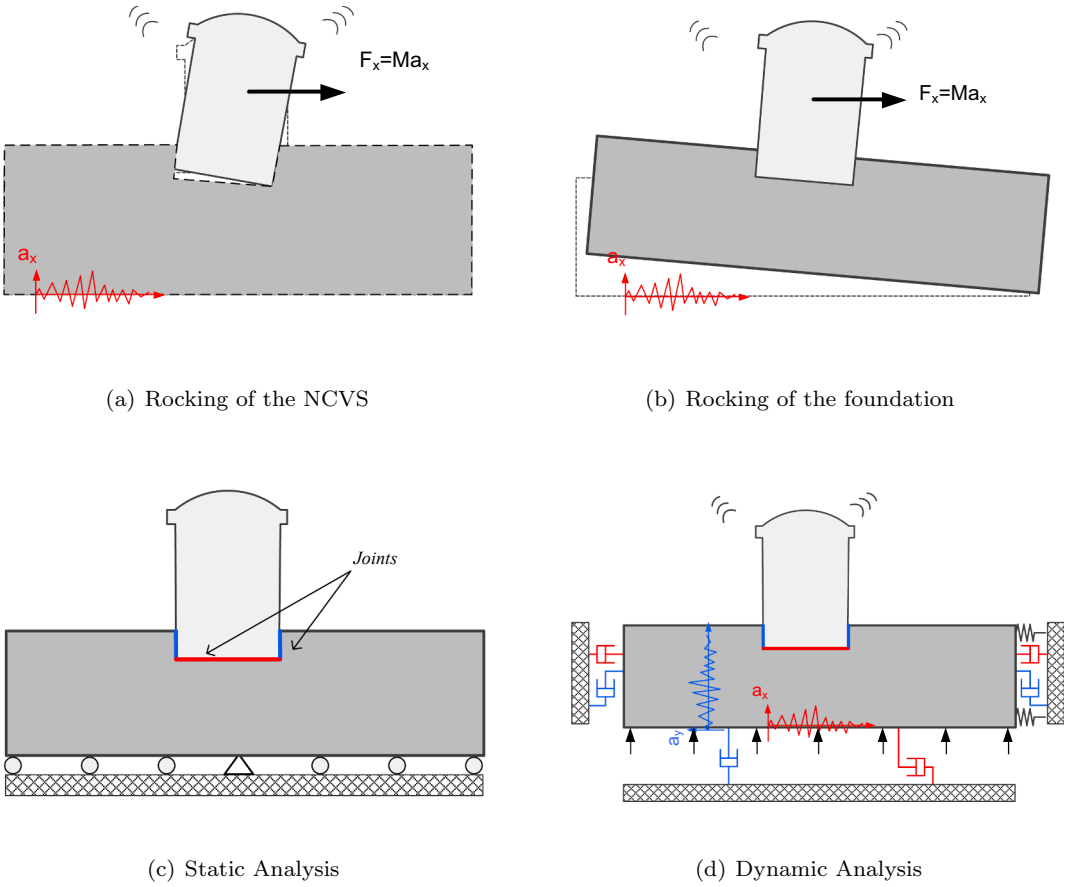

Fig. 5. Potential rocking and two part analyses to mitigate rocking, radiation damping and rigid body motion.

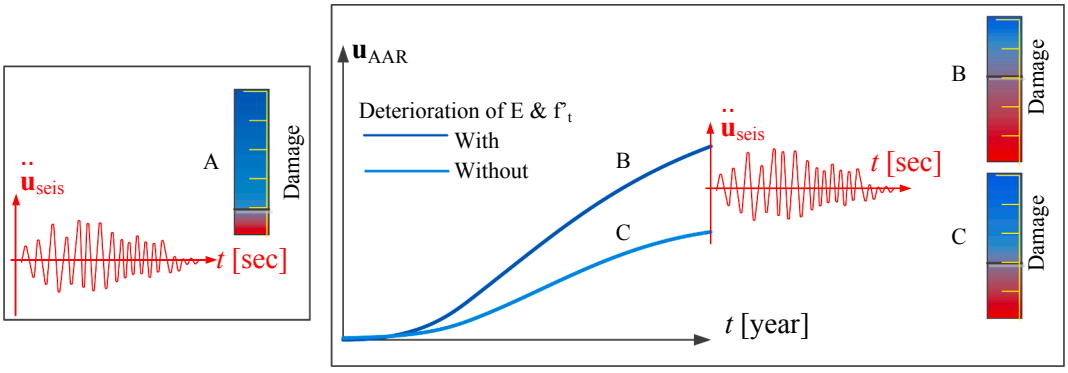

Fig. 6. Three scenarios of investigation: A: No ASR; B: ASR with 40% damage; and C: ASR without Damage.

subjected to ASR (as a result of the high relative humidity likely to be present in the surrounding foundation). Material properties are separately shown in Appendix sA.

The potential secondary stresses induced by the uplift forces (caused by the eccentricity of the resulting inertial force), Fig. 7(b), will be mitigated by the insertion of cohesive based joint elements (Cervenka et al., 1998) where necessary. A 3D continuum model, Fig. 7(c) is prepared. Reinforcement is modeled as "smeared" by altering the stiffness matrices of those continuum elements they cross. A 0.5% reinforcement was assumed in both directions.

Different material groups are defined in the FE model. Concrete was modeled by four distinct groups according to location, mesh densities, and whether it is reactive, Fig. 7. The dome is assumed to be linear elastic, whereas the wall and the base are modeled as nonlinear using the well-tested smeared crack model (Cervenka and Papanikolaou, 2008) of the FE code ATENA (Červenka and Jendele, 2016).

ASR is captured by the constitutive model described above, (Saouma and Perotti, 2006). It is assumed that the NCVS operates for 40 years during which it undergoes a relatively mild total expansion of 0.3% uniformly distributed over the "contaminated" zone as an additional internal strain. In actuality, ASR is not so uniform and is more likely to be "spotty" to reflect the usage of reactive aggregates in some, but not all the pours. This stochastic process is not accounted for in this study, however a separate study indicates that a sparsely distributed ASR expansion may be more detrimental than a uniformly distributed one (due to the induced strain discontinuities) (Hariri-Ardebili et al., 2018). Accompanying this expansion are two levels of concrete degradation zero and 30% reduction of E and f_t' after 40 years. The 40 years expansion is simulated in two weeks increments assuming a constant temperature and RH. The external average temperature at the site is estimated to be 11°C (external face of NCVS), the internal temperature is in turn estimated to be 25°C. Hence, an average mean yearly

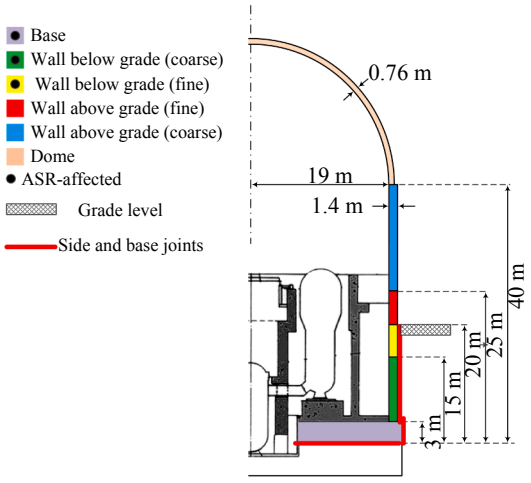

(a) Geometry and dimensions

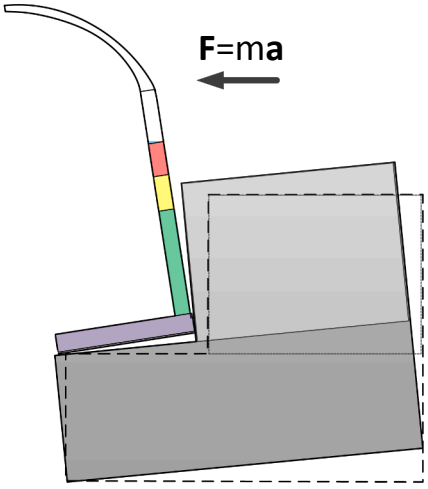

(b) Potential uplift modeled by joint elements

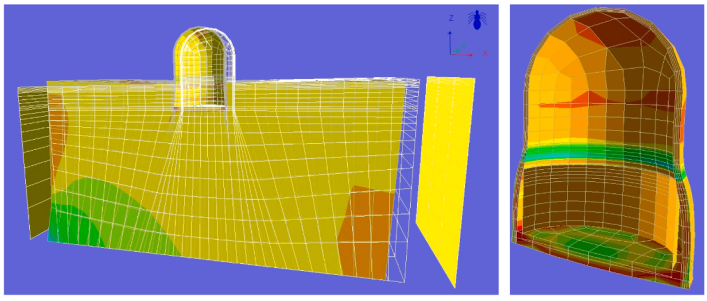

(c) Half 3D model with lateral viscous dampers and container mesh (with ASR expansion)

Fig. 7. Geometry, material groups, role of joint elements, and finite element mesh.

temperature of $(25 + 11)/2 = 18$ °C is assumed. Note that in a more refined analysis, the temperature distribution across the wall should be considered, and monthly average temperatures should also be refined.

Rock (both the foundation and lateral) is assumed to be linear elastic. Interface joints are placed around and below the NCVS to capture potential uplift of lateral separation of the container from the adjacent rock.

3.3.2. Stochastic seismic excitations

Selection of the "right" earthquake records is a critical (and often underestimated) task. A multi-step approach is followed:

1. Site Characteristics are first determined assuming that the NCVS is located in New Hampshire, USA (coordinates $42°53'56''N$ and $70°51'03''W$). The corresponding site conditions are then estimated from the *opensha* code (Field et al., 2003) which requires V_{S30} (shear wave velocity 30 m below the surface) determined from the topographic slope site classification map method (Wald and Allen, 2007), Fig. 8(a).
2. The seismic hazard de-aggregation (probability of occurrence in terms of distance and magnitude of earthquake) is determined next. Using the USGS 2008 *Interactive Deaggregations service* (USGS 2003,), the modal distance (R), magnitude (M), and inter-event term (ϵ_0) contributing to the 50%/50 yr shaking are computed. Fig. 8(b) shows a de-aggregation seismic hazard plot where peaks correspond to magnitude-distance combinations that contribute more to the hazard. This was determined from[3] USGS (2017).
3. Collecting a set of ground motion records is the last step. Ground motions are either selected (PEER ground-motion database is used in most of the cases (PEER, 2017)) or artificially generated. As already stated, two stochastic techniques are used in this paper:
   (a) ETAFs: Six different randomly generated ETAFs, with main characteristics previously explained were used. Schematically, all the ETAFs are analogous Fig. 4(a) as the base of all of them is a random white noise.
   (b) Stochastic Ground motions: Two scenarios, based on Fig. 8(b), were considered: a) S1: $\langle M = 7.0, R = 10\rangle$, Fig. 9; and b) S2: $\langle M = 5.5, R = 50\rangle$, Fig. 9(b); where M refers to the magnitude, and R the distance. In both cases a total of $N_{sim} = 25$ samples are selected to properly address the record-to-record (RTR) variability. S1 scenario is stronger than S2, and thus, more damage is expected for that. All generated (Rezaeian and Der Kiureghian, 2008) ground motions were far-field resulting from a strike-slip fault, and a shear wave velocity V_{S30} of 760 m/s.

3.4. Results

Analysis was performed by the code Merlin (Saouma et al., 2010)

[3] The site was being upgraded in the Fall 2017, and subsequent results are not exactly the corresponding ones.

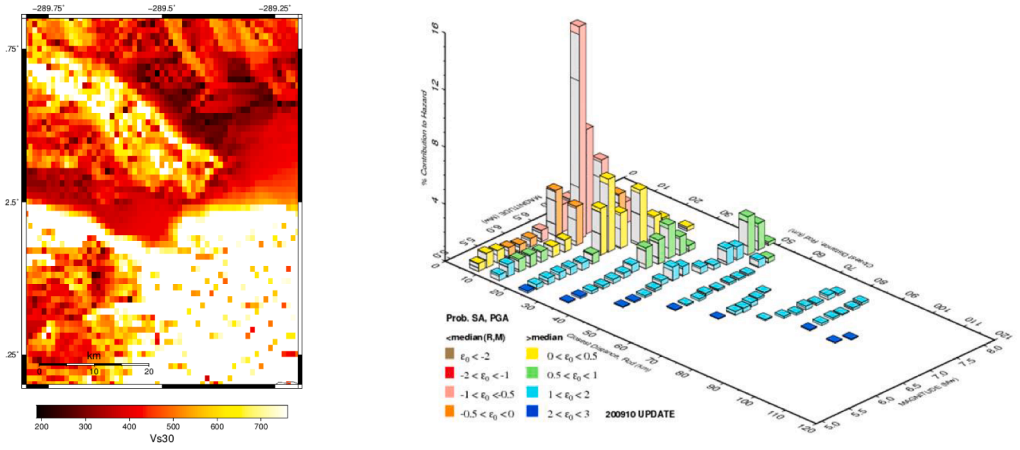

(a) Map of estimated V_{S30} (b) Seismi de-aggregation

Fig. 8. Seismic hazard characterization around the nuclear site.

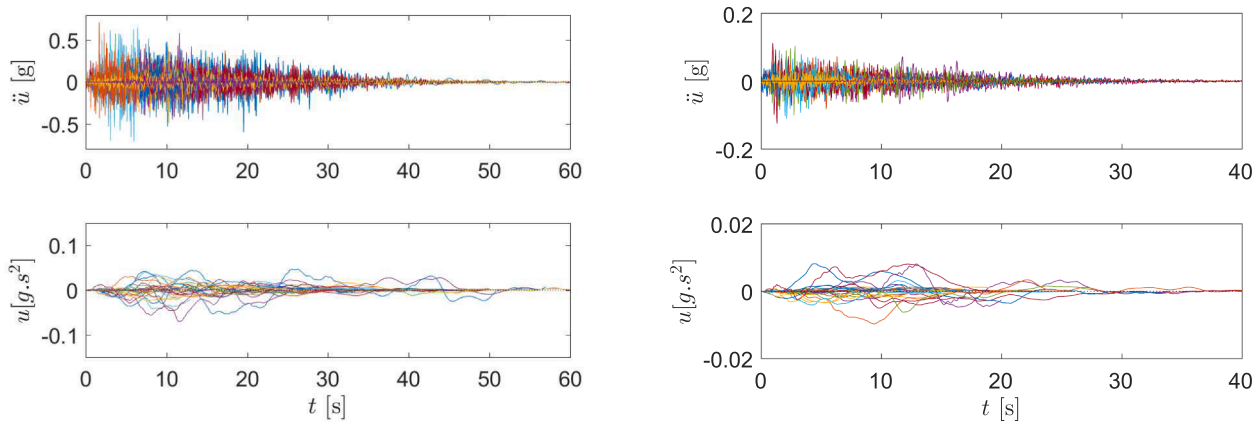

(a) S1 $< M = 7.0, R = 10 >$ (b) S2 $< M = 5.5, R = 50 >$

Fig. 9. Acceleration and displacement time history of 25 random signals for each scenario.

which to the best of the authors knowledge is the only code that has been "validated" by performing nearly all the analyses proposed by the RILEM (Saouma et al., 2017). Three sets of analyses were performed: 1) Static + ASR, 2) Static + Dynamic, and 3) Static + ASR + Dynamic (100 for the stochastic ground motions, and three for each of the six ETA).

3.4.1. Static + ASR analyses

In this first analysis, 40 years of ASR in the NCVS is simulated. Fig. 10(a) shows swelling of the container along with a closeup on the concrete-rock separation. Clearly ASR expansion interacts with the structure in what may be *a priori* counter-intuitive: a) the mat expands in a concave shape due to the structural constraints of the cylindrical vessel, Fig. 10(b)-1; b) the wall pushes against the adjacent rock, but is constrained by both the base mat and the upper portion of the enclosure not subjected to expansion, Fig. 10(b)-2, causing strong curvature, joint opening, and ensuing stress discontinuities; and c) sliding of the NCVS itself, Fig. 10(b)-3. Furthermore, the evolution of concrete cracks is shown in Fig. 10(c). It should be noted that cracking starts at the central region of the mat base and along a ring on the wall next to soil level.

3.4.2. Impact of ASR on capacity curves: ETA method

Impact of ASR on the structural response of the NCVS can now be ascertained by comparing "Static + Seismic" with "Static + ASR + Seismic" for displacement and stresses for six different ETA functions. Three sets of simulations are compared: a) Static + dynamic analysis (Referred to Dyn. in the plots); b) Static + ASR with degradation of f_t' and E over time + dynamic analysis; and c) Static + ASR (without material degradation) + dynamic analysis.

Displacements: The absolute value of the (horizontal) displacements corresponding to peaks in (the six) ETAFs is first extracted. Eq. (6) is used to determine the maximum QoI (i.e. displacement). The mean of those six ETAFs for each of three assumptions are computed, Fig. 11(a). These are ramping curves as the dynamic acceleration is indeed defined as a linearly increasing one (Fig. 4(a)). To better grasp the impact of ASR, results are normalized with respect to the one without ASR (dynamic only), Fig. 11(b). The deviations are time-dependent and, as expected, model with ASR degradation is much more impacted than the one without. On average, and for this case study, ASR with degradation results in ~20% change, whereas the one without has ~8% variation with respect to the "Dyn. only" model. If material degradation is ignored (which is an erroneous abstraction) displacements are still lower than those cases without ASR, but greater than ASR with degradation. Note that discrepancy with respect to the case without ASR starts at around 9 s (i.e., until this point the ASR had little impact on deformation). The impact of ASR (with and without degradation) is time-dependent due to the complexities of the internal stress states induced by it or resulting from the seismic excitation,

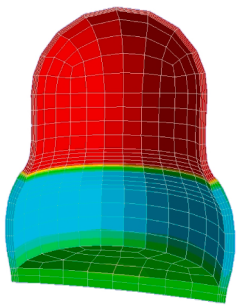

(a) Swelling of contaminated zone

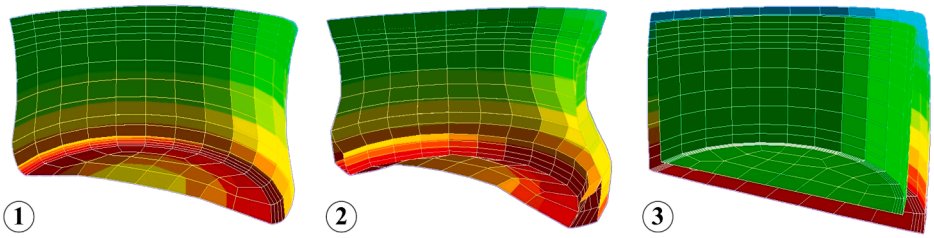

(b) Evolution of joint opening/sliding due to ASR

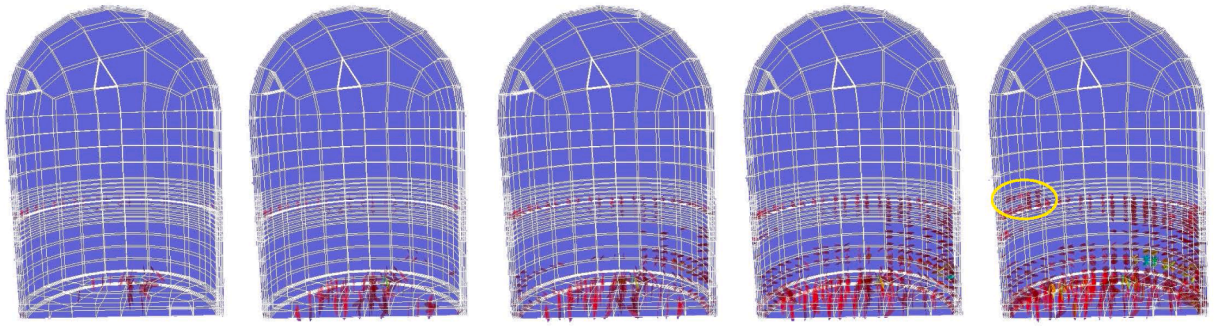

(c) Internal crack propagation (left to right)

Fig. 10. Response of NCVS under static + ASR analysis after 40 years.

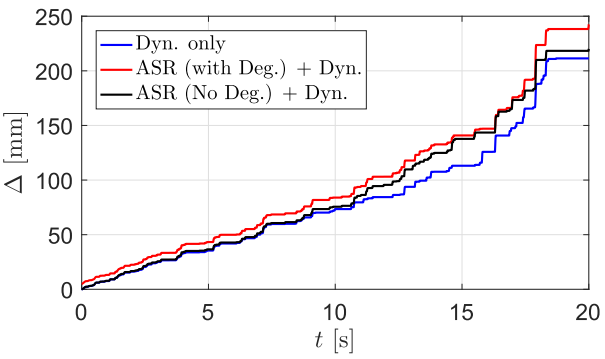

(a) Displacement profile at the top

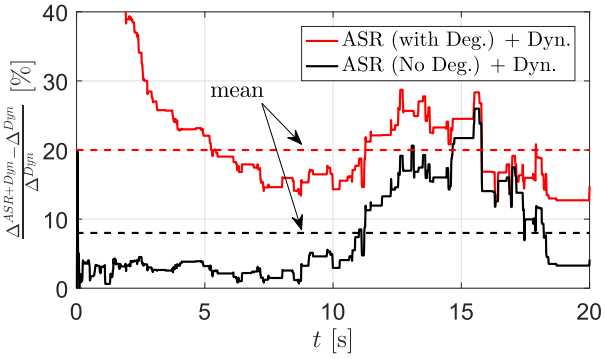

(b) Displacements normalized and mean differences

Fig. 11. ETA-based displacements and the mean differences.

Fig. 11(b).

Stresses: Time history of maximum principal stresses are recorded. The ASR affected responses result in higher stresses than those without degradation, and additional substantial damages will be induced by the ASR (with internal damage accounted for). At the base, Fig. 12(a), maximum principal stresses are positive (cracking) and attenuate with time. Stresses are at first low when ASR dominates, but then suddenly increase with a localized damage at time ≃17 s. At the grade elevation, Fig. 12(b), stresses are much higher without ASR, and then gradually decrease with no indication of failure. Note that the tensile strength is 3.1 MPa. On the other hand, in the presence of prior ASR expansion, the stresses are negative, and a sudden localized failure appears at $t = 14$ s. For a point above grade, Fig. 12(c), stresses are higher in the absence of ASR and there is indication of a localized failure at $t = 15$ s. In the presence of ASR, the failure is delayed to about 17 s. Finally, at the base of the dome, Fig. 12(d), the ASR stresses are substantially higher than without and localized failure occurs around 17 s. For this case, ASR has reduced the stresses at the base, but substantially increased them at the base of the dome. Indeed, stress attenuation with time is the direct result of a nonlinear analysis where upon cracking there is a substantial stress redistribution resulting in localized stress reduction.

Cracking: of the structure is shown Fig. 13 at different times. In general, the crack pattern of ASR affected models are different and the previous observations are qualitatively confirmed by the crack profiles. Indeed, the damage index (DI), ratio of the cracked sections to the total area, is highest when ASR (with damage) preceded the seismic

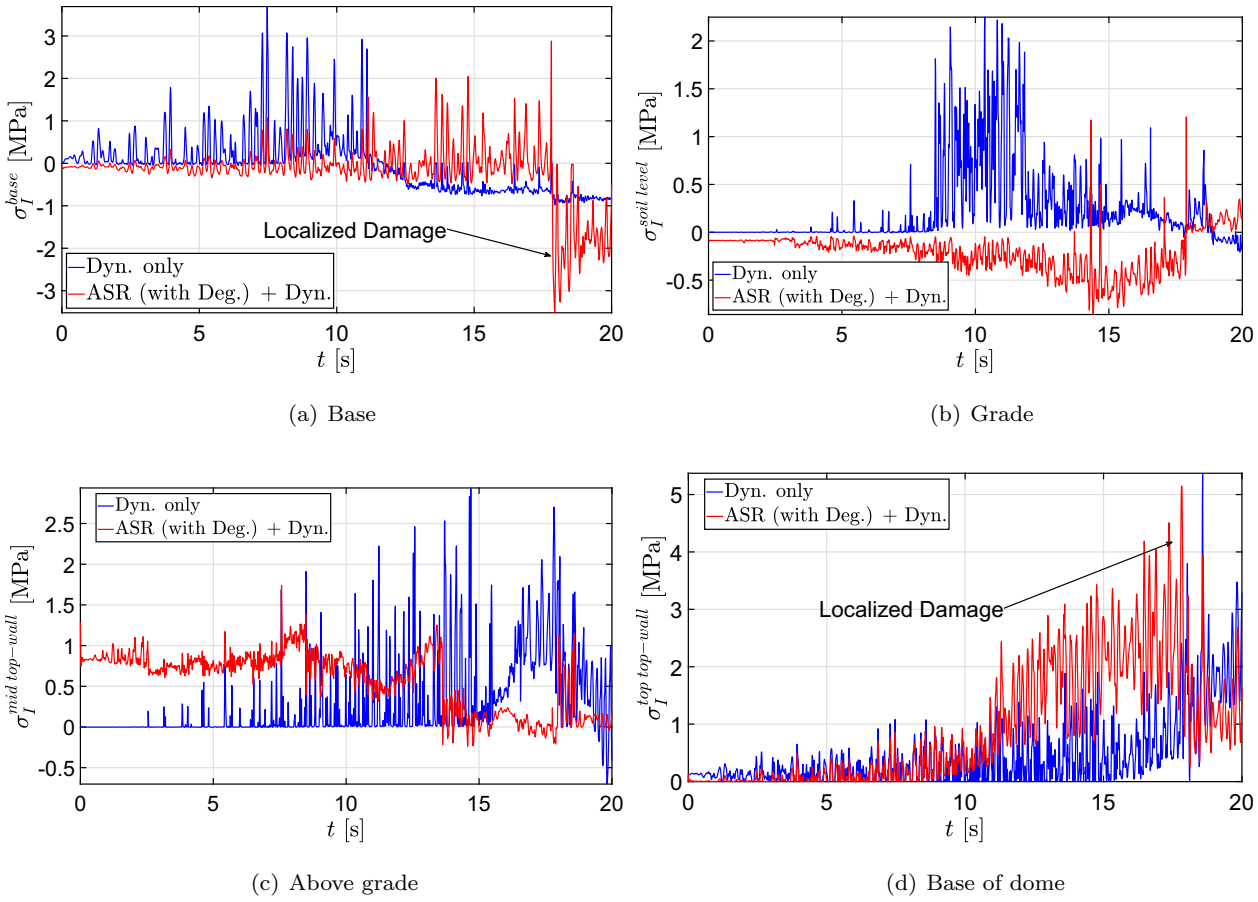

(a) Base (b) Grade

(c) Above grade (d) Base of dome

Fig. 12. Principal stresses capacity curves.

excitation. The ASR has a much higher impact of that portion of the NCVS below grade than above (where no ASR is modeled).

The sound NCVS experiences the major cracks at the soil level at about 12.8 s, while at the corresponding time the ASR-affect NCVS had already some major cracks though all the top-wall. Results of ETA analysis prove that "endurance" of the NCVS is reduced when it is subjected to initial ASR.

3.4.3. Impact of ASR on fragility curves: stochastic analysis

As previously mentioned, two scenarios are selected, S1 and S2 and for each one, 25 random ground motions are generated. Then, each set is applied to the virgin NCVS (i.e. without ASR) and then to the ASR affected one (with material degradation). Thus, a total of $4 \times 25 = 100$ simulations are performed.

Although it is possible to perform the fragility analysis based on various QoIs, the displacement response is selected as: 1) it is a global metric capturing the structural response; and 2) it is simple and straightforward to use in the probabilistic model.

Figs. 14(a) and (c) show the peak displacements for each of the 25 stochastic ground motions versus the PGA for scenario S1 ($\langle M = 7.0, R = 10\rangle$) and S2 ($\langle M = 5.5, R = 50\rangle$), respectively. These figures call for the following observations: a) The minimum intensity of the records in S1 group (PGA $\sim$0.13 g) is nearly identical to the maximum PGA in S2; b) Relative displacements (with respect to the base) Δ_{max} in S1 is distributed between 5 and 55 mm, while in S2 they range from 1 to 10 mm (with only one exception at about 16 mm); and c) For the lower intensity case (S2), displacements of ASR affected NCVS are consistently higher than sound ones, however for the higher intensity (S1), 5 out of 25 models show lower displacements for ASR-affected NCVS.

Fragility curves, Eq. (9), require a limit state (LS) value (by *QoI* in the equation). Ideally, this should be a concrete crack opening. Should the steel liner leak tightness be also jeopradized, then and only then there could be leakage. However, such LS are not codified in nuclear engineering (as opposed to relative drifts for instance for buildings). Hence, and due to software current limitation, a displacement based LS at the top of the dome was adopted and values arbitrarily assumed (and shown in the respective figures). Resulting fragility curves are shown in Fig. 14(b) and (d). For scenario S2, the probability of exceedance of a specific LS function is always higher for ASR-affected NCVS. On the other hand, under scenario S1, the impact of ASR on the probability of exceedance is much smaller than under scenario S2. This would imply that ASR has a higher impact for low intensity earthquake events (such as design based earthquakes) than for high ones (associated with the low probability events used in an SPRA).

Finally, when both the ground motion intensity and the LS threshold are not known, then a corresponding fragility surface combining the two parameters can be generated to address the increased uncertainties, Fig. 15.

4. Summary and conclusions

This paper was an attempt to perform a modern analysis by integrating advanced computational models for ASR, seismic hazard analysis, nonlinear structural analysis, soil-structure interaction, and damage analysis resulting in fragility and capacity curves. The major limitation of this study is the adoption of a displacement-based limit state whereas a crack opening (facilitating leak) would have been more appropriate.

The major conclusion of this paper is that ASR will undoubtedly impact the safety of a structure. That impact will increase with a decrease in the ground motion intensity. This would imply that ASR can

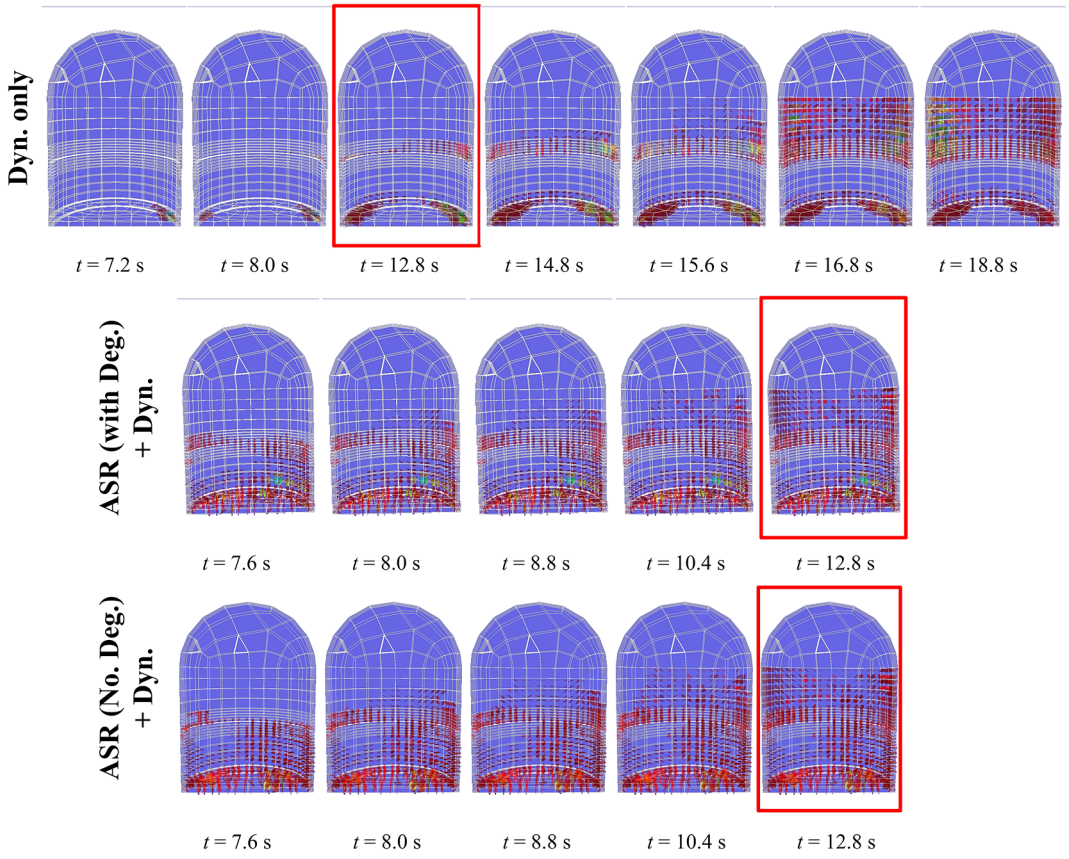

Fig. 13. Crack profile from a sample ETA simulation at identical time steps.

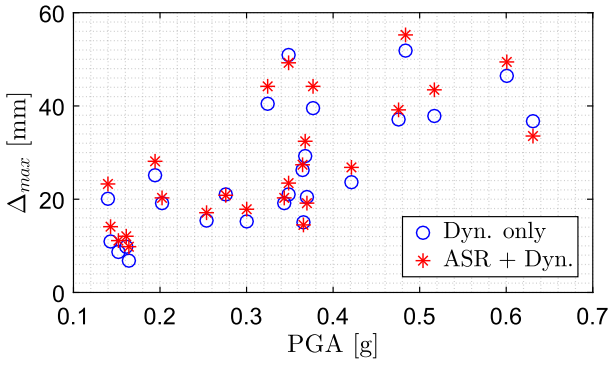

(a) Raw data for S1 ($M = 7.0$)

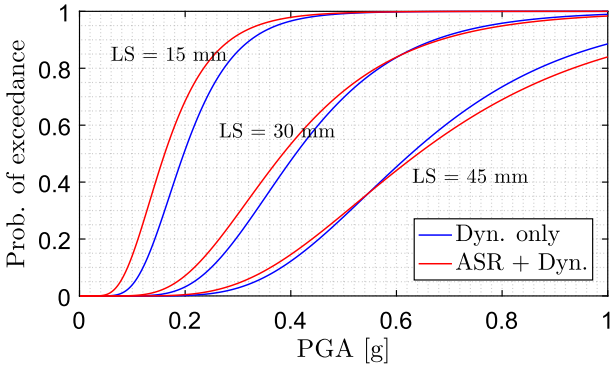

(b) Fragility curves for S1

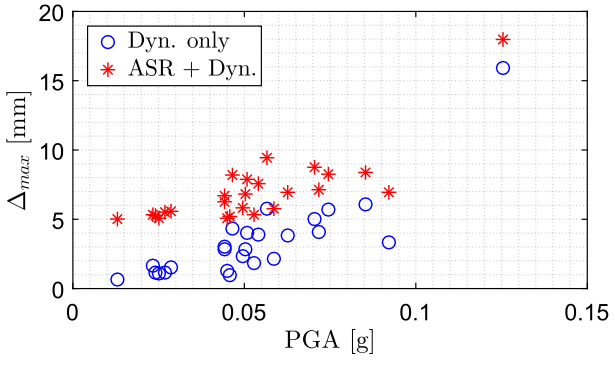

(c) Raw data for S2 ($M = 5.5$)

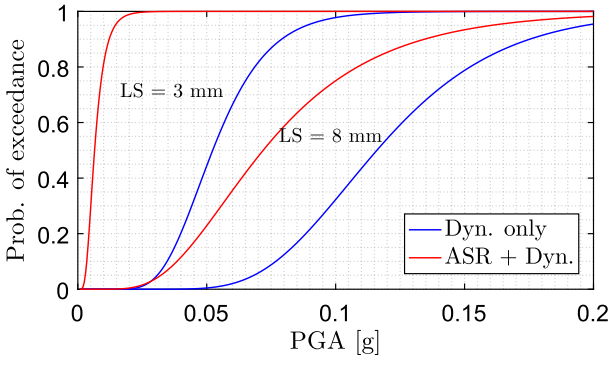

(d) Fragility curves for S2

Fig. 14. Displacement-based fragility curves.

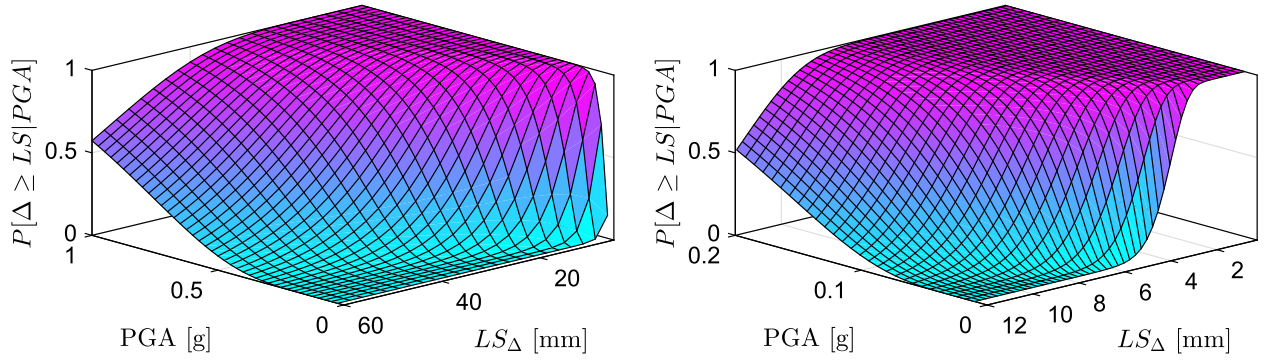

(a) Scenario S1 (b) Scenario S2

Fig. 15. Displacement-based fragility surfaces.

be more damaging for a design base earthquake than for higher intensity one associated with an SPRA.

Acknowledgment

The authors would like to acknowledge the partial financial support of the U.S. Nuclear Regulatory Commission (Madhumita Sircar Technical Analyst) to the University of Colorado (Boulder) through Grant No. NRC-HQ-60-14-G-0010.

The views and opinions expressed are those of the authors and do not necessarily reflect the official position of the Nuclear Regulatory Commission. Examples of analyses performed within this paper are only examples, they should not be utilized in real-world analytic products as they may be based only on very limited and dated open source information.

The numerous and constructive comments of the two anonymous reviewers were very helpful in greatly improving this manuscript. In particular the input of one reviewer in addressing the contextual framework of the SPRA is greatly appreciated.

Appendix A. Material properties

.

Appendix B. Performance based earthquake engineering

Interestingly, what started with the nuclear industry was subsequently embraced by the building community under the label of Performance Based Earthquake Engineering. By analogy, FEMA P-750 (2009) provides minimum recommended requirements necessary for the design and construction of new buildings to resist earthquake ground motions, and to provide reasonable assurance of seismic performance. Applied Technology Council (2012) describes a general methodology and recommended procedures to assess the probable seismic performance of individual buildings. Performance is measured in terms of the probability of incurring casualties, repair and replacement costs, repair time, and unsafe placarding. The methodology and procedures are applicable to new or existing buildings, and can be used to: (1) assess the probable performance of a building; (2) design new buildings to be capable of providing desired performance; or (3) design seismic upgrades for existing buildings to improve their performance. Finally, Deierlein et al. (2010) is a guide for practicing engineers for the nonlinear structural analysis for seismic design.Table A.1, Table A.2, Table A.3.

An incomplete comparison between SPRA and PBEE is shown in Table A.4. It should be noted that SSI and rocking (addressed below) should be included as part of and SPRA, and that only PBEE requires nonlinear analysis for a full assessment.

Table A.1
Concrete mechanical properties.

Characteristics	Symbol	Unit	Base	Wall below	Wall above	Dome
Mass density	ρ	Gg/m^3	0.002250	0.002250	0.002250	0.002250
Modulus of elasticity	E	MPa	39,000	39,000	39,000	39,000
Poisson's ratio	ν	–	0.2	0.2	0.2	0.2
Tensile strength	f_t	MPa	3.1	3.1	3.1	3.1
Fracture energy (Exponential softening)	G_F	MN/m	1.2e−4	1.2e−4	1.2e−4	1.2e−4
Compressive strength	f_c	MPa	−31.0	−31.0	−31.0	−31.0
Critical displacement in compression	w_d	m	−0.0005	−0.0005	−0.0005	−0.0005
Factor beta for return direction	β	–	0.0	0.0	0.0	0.0
Factor e for roundness of failure surface	e	–	0.55	0.55	0.55	0.55
Onset of nonlinearity in compression	f_{c0}	MPa	−20.0	−20.0	−20.0	−20.0
Plastic strain at compressive strength	ϵ_{cp}	–	−1e−3	−1e−3	−1e−3	−1e−3

Table A.2
Characteristics of the ASR model.

Characteristics	Symbol	Unit	Base	Wall
Reference temperature	T_0	–	18	18
Maximum volumetric expansion at T_0^{test}	$\varepsilon_{ASR}^{\infty}$	–	0.3%	0.3%
Characteristic time at T_0^{test}	τ_C	ATU	64	64
Latency time at T_0^{test}	τ_L	ATU	160	160
Activation energy for τ_C	U_C	–	5400	5,400
Activation energy for τ_L	U_L	–	9400	9,400
Residual reduction factor	Γ_r	–	0.5	0.5
Fraction of ε_t prior to reduction of ASR expansion due to macro cracking	γ_t	–	0.5	0.5
ASR expansion annealing stress	σ_U	MPa	−8	−8
Post-ASR residual relative Young modulus	β_E	–	70%	70%
Post-ASR residual tensile strength	β_{f_t}	–	70%	70%

Table A.3
Rebar mechanical properties.

Characteristics	Symbol	Unit	Vertical	Horizontal
reinforcement ratio	ρ	–	0.01	0.005
Modulus of elasticity	E	MPa	200,000	200,000
Poisson's ratio	ν	–	0.3	0.3
Yield stress	σ_Y	MPa	248	248

Table A.4
Analogy between nuclear and building safety guidelines.

Nuclear SPRA	Building PBEE
Relevant documents	
Kennedy and Ravindra (1984)	
Asme (2015)	FEMA P-750 (2009)
ASCE/SEI 43-05 (2005)	Applied Technology Council (2012)
ASCE 4-16 (2016)	Deierlein et al. (2010)
Steps	
1. Seismic hazard evaluation	1. Hazard Analysis → Intensity measure (IM) 2. Structural Analysis → Engineering demand parameter (EDP)
2. Component fragility evaluation	3.Damage analysis → Damage measure (DM); fragility curves
3. Plant system and accident sequence analysis	4. Loss analysis → Decision variable (DV)
4. consequence analysis	

Appendix C. Supplementary data

Supplementary data associated with this article can be found, in the online version, at https://doi.org/10.1016/j.nucengdes.2019.02.011.

References

ACI 318-14, 2014. Building Code Requirements for Structural Concrete (ACI 318-14) and Commentary. American Concrete Institute Technical report.

ADAMS Accession No, M.A., 2012. Order Modifying Licenses With Regard To Requirements For Mitigation Strategies For Beyon D-+Design-+Basis External Events (Effective Immediately).

Applied Technology Council, 2012. Seismic performance assessment of buildings volume 1 – methodology. Federal Emergency Management Agency Technical Report FEMA P-58-1.

Ares, A.F., Fatehi, A., 2013. Development of probabilistic seismic hazard analysis for international sites, challenges and guidelines. Nucl. Eng. Des. 259, 222–229.

ASCE 4-16, 2016. Seismic Analysis of Safety-Related Nuclear Structures. Technical report. American Society of Civil Engineers.

ASCE/SEI 43-05, 2005. Seismic Design Criteria for Structures, Systems, and Components in Nuclear Facilities. American Society of Civil Engineers, Reston, VA.

Ashar, H., Scott, B., Artuso, J.F., Stevenson, J.D., 2001. Code for concrete reactor vessels and containments. ASME Boiler & Pressure Vessel Code, Sec. III 504 (2).

Asme III, B., 2015. BPVC Section III-Rules for Construction of Nuclear Facility Components-Division 2-Code for Concrete Containments. Technical report. American Society of Mechanical Engineering.

Baker, J., 2015. Efficient analytical fragility function fitting using dynamic structural analysis. Earthquake Spectra 31 (1), 579–599.

Baušys, R., Dundulis, G., Kačianauskas, R., Markauskas, D., Rimkevičius, S., Stupak, E., Stupak, S., Šliaupa, S., 2008. Sensitivity of dynamic behaviour of the FE model: case study for the ignalina NPP reactor building. J. Civil Eng. Manage. 14 (2), 121–129.

Beckjord, E.S., Cunningham, M.A., Murphy, J.A., 1993. Probabilistic safety assessment development in the united states 1972-1990. Reliab. Eng. Syst. Saf. 39 (2), 159–170.

Ben-Ftima, M., Sadouki, H., Bruhwiler, E., 2016. Development of a computational multi-physical framework for the use of nonlinear explicit approach in the assessment of concrete structures affected by alklai-aggregate reaction. In: Saouma, V., Bolander, J., Landis, E. (Eds.), 9th International Conference on Fracture Mechanics of Concrete and Concrete Structures. FraMCoS-9, Berkeley, CA.

Bradley, B.A., Pettinga, D., Baker, J.W., Fraser, J., 2017. Guidance on the utilization of earthquake-induced ground motion simulations in engineering practice. Earthquake Spectra 33 (3), 809–835.

Braverman, J., Miller, C., Hofmayer, C., Ellingwood, B., Naus, D., Chang, T., 2004.

Degradation assessment of structures and passive components at nuclear power plants. Nucl. Eng. Des. 228 (1), 283–304.
Cervenka, J., Chandra, J., Saouma, V., 1998. Mixed mode fracture of cementitious bi-material interfaces; Part ii: Numerical simulation. Eng. Fract. Mech. 60 (1), 95–107.
Cervenka, J., Papanikolaou, V., 2008. Three dimensional combined fracture-plastic material model for concrete. Int. J. Plast 24 (12), 2192–2220.
Červenka, V., Jendele, L., 2016. Atena program documentation part.
Chen, J., Zhao, C., Xu, Q., Yuan, C., 2014. Seismic analysis and evaluation of the base isolation system in AP1000 NI under SSE loading. Nucl. Eng. Des. 278, 117–133.
Chénier, J., Komljenovic, D., Gocevski, V., Picard, S., Chrétien, G., 2012. An approach regarding aging management program for concrete containment structure at the gentilly-2 nuclear power plant. In: Proceedings of 33rd Annual Conference of the Canadian Nuclear Society. TCU Place, Saskatoon, Saskatchewan, Canada, pp. 126 volume 1013.
Choi, I.-K., Choun, Y.-S., Ahn, S.-M., Seo, J.-M., 2008. Probabilistic seismic risk analysis of candu containment structure for near-fault earthquakes. Nucl. Eng. Des. 238 (6), 1382–1391.
Choi, I.-K., Choun, Y.-S., Seo, J.-M., 2003. Scenario earthquakes for korean nuclear power plant site considering active faults. In: XVII International Conference on Structural Mechanics in Reactor Technology. Czech Republic, August, Prague, pp. 17–22.
Coleman, J.L., Bolisetti, C., Whittaker, A.S., 2016. Time-domain soil-structure interaction analysis of nuclear facilities. Nucl. Eng. Des. 298, 264–270.
Comi, C., Fedele, R., Perego, U., 2009. A chemo-thermo-damage model for the analysis of concrete dams affected by alkali-silica reaction. Mech. Mater. 41 (3), 210–230.
Cornell, A., Jalayer, F., Hamburger, R., 2002. Probabilistic basis for 2000 SAC federal emergency management agency steel moment frame guidelines. J. Struct. Eng. 128, 526–532.
De Grandis, S., Domaneschi, M., Perotti, F., 2009. A numerical procedure for computing the fragility of npp components under random seismic excitation. Nucl. Eng. Des. 239 (11), 2491–2499.
Deierlein, G.G., Reinhorn, A.M., Willford, M.R., 2010. Nonlinear structural analysis for seismic design; a guide for practicing engineers. National Institute of Science and Technology (NIST) report GCR 10-917-5.
Desai, S.S., Choudhury, D., 2015. Site-specific seismic ground response study for nuclear power plants and ports in mumbai. Nat. Hazard. Rev. 16 (4), 04015002.
Dolšek, M., 2012. Simplified method for seismic risk assessment of buildings with consideration of aleatory and epistemic uncertainty. Struct. Infrastruct. Eng. 8, 939–953.
Ebisawa, K., Ando, K., Shibata, K., 2000. Progress of a research program on seismic base isolation of nuclear components. Nucl. Eng. Des. 198 (1-2), 61–74.
El Mohandes, F., Vecchio, F., 2013. VecTor3: A. User's Manual; B. Sample Coupled Thermal and Structural Analysis. Dept. of Civil Engineering, University of Toronto, Toronto, Canada.
Ellingwood, B.R., 1998. Issues related to structural aging in probabilistic risk assessment of nuclear power plants. Reliab. Eng. Syst. Saf. 62 (3), 171–183.
EPRI, 2000. Individual Plant Examination for External Events (IPEEE) Seismic Insights. Electric Power Research Institute, pp. 1000895 Technical report.
EPRI, 2003. Seismic Probabilistic Risk Assessment Implementation Guide. Electric Power Research Institute, pp. 3002000709 Technical report.
EPRI, 2013. Seismic Evaluation Guidance: Augmented Approach for the Resolution of Fukushima Near-Term Task Force Recommendation 2.1 – Seismic. Technical Report 3002000704. Electric Power Research Institute, Palo-Alto, CA.
EPRI, 2017. Modeling existing concrete containment structures: Lessons learned. Technical report. Electric Power Research Company 58 pages.
Estekanchi, H., Valamanesh, V., Vafai, A., 2007. Application of endurance time method in linear seismic analysis. Eng. Struct. 29 (10), 2551–2562.
Farmer, F.R., 1967. Reactor Safety and Siting: A Proposed Risk Criterion. United Kingdom Atomic Energy Authority, Risley, Eng Technical report.
FEMA P-750, 2009. Nehrp recommended seismic provisions for new buildings and other structures (fema p-750). Federal Emergency Management Agency, Washington, DC.
Field, E., Jordan, T., Cornel, C., 2003. Opensha: a developing community-modeling environment for seismic hazard analysis. Seismol. Res. Lett. 74, 406–419.
Frano, R.L., Pugliese, G., Forasassi, G., 2010. Preliminary seismic analysis of an innovative near term reactor: methodology and application. Nucl. Eng. Des. 240 (6), 1671–1678.
Graves, H., Le Pape, Y., Naus, D., Rashid, J., Saouma, V., Sheikh, A., Wall, J., 2013. Expanded materials degradation assessment (EMDA). In: Ageing of concrete. Technical Report NUREG/CR-ORNL/TM-2011/545, vol. 4 U.S. Nuclear Regulatory Commission.
Guimarães, A.C.F., Cabral, D.C., Lapa, C.M.F., 2006. Adaptive fuzzy system for degradation study in nuclear power plants' passive components. Progr. Nucl. Energy 48 (7), 655–663.
Hakata, T., 2004. Computer model for coincidental failure of nuclear power plants due to seismic events in a multi-unit site. In: Probabilistic Safety Assessment and Management. Springer, pp. 1245–1251.
Hakata, T., 2007. Seismic PSA method for multiple nuclear power plants in a site. Reliab. Eng. Syst. Saf. 92 (7), 883–894.
Hardy, G., Richards, J., Mauer, A., Kassawara, R., 2015. Us nuclear power industry post-fukushima seismic response initiatives. In: Proceedings of the 23rd Conference on Structural Mechanics in Reactor Technology, Manchester, United Kingdom.
Hariri-Ardebili, M., Furgani, L., Meghella, M., Saouma, V., 2016. A new class of seismic damage and performance indices for arch dams via eta method. Eng. Struct. 110, 145–160.
Hariri-Ardebili, M., Saouma, V., 2016. Sensitivity and uncertainty quantification of the cohesive crack model. Eng. Fract. Mech. 155, 18–35.
Hariri-Ardebili, M., Saouma, V., 2017. Single and multi-hazard capacity functions for concrete dams. Soil Dyn. Earthquake Eng. 101, 234–249.
Hariri-Ardebili, M., Saouma, V., 2018. Sensitivity and uncertainty analysis of AAR affected shear walls. Eng. Struct. 172, 334–435.
Hariri-Ardebili, M., Saouma, V., Merz, C., 2018. Risk-informed conditional assessment of a bridge with alkali aggregate reaction. ACI Struct. J. 115 (2), 475–487.
Hariri-Ardebili, M., Saouma, V., Porter, K., 2016. Quantification of seismic potential failure modes in concrete dams. Earthquake Eng. Struct. Dynam.
Hariri-Ardebili, M., Sattar, S., Estekanchi, H., 2014. Performance-based seismic assessment of steel frames using endurance time analysis. Eng. Struct. 69, 216–234.
Hessheimer, M.F., Dameron, R.A., 2006. NUREG/CR-6906 SAND2006-2274P: Containment Integrity Research at Sandia National Laboratories; An Overview.
Hoseyni, S.M., Yousefpour, F., Araei, A.A., Karimi, K., Hoseyni, S.M., 2014. Effects of soil-structure interaction on fragility and seismic risk; a case study of power plant containment. J. Loss Prev. Process Ind. 32, 276–285.
Huang, H., Spencer, B., 2016. Grizzly model for fully coupled heat transfer, moisture, diffusion, alkali-silica reaction and fractureing process in concrete. In: Saouma, V., Bolander, J., Landis, E. (Eds.), 9_{th} International Conference on Fracture Mechanics of Concrete and Concrete Structures. FraMCoS-9, Berkeley, CA.
Huang, H., Spencer, B., Cai, G., 2015. Grizzly model of multi-species reactive diffusion, moisture/heat transfer, and alkali-silica reaction in concrete. Technical Report INL/EXT-15-36425. Idaho National Laboratory, Idaho Falls, Idaho 83415.
Huang, X., Kwon, O.-S., Bentz, E., Tcherner, J., 2017. Evaluation of CANDU NPP containment structure subjected to aging and internal pressure increase. Nucl. Eng. Des. 314, 82–92.
Huang, Y.-N., Whittaker, A.S., Kennedy, R.P., Mayes, R.L., 2013. Response of base-isolated nuclear structures for design and beyond-design basis earthquake shaking. Earthquake Eng. Struct. Dyn. 42 (3), 339–356.
Huang, Y.-N., Whittaker, A.S., Luco, N., 2010. Seismic performance assessment of base-isolated safety-related nuclear structures. Earthquake Eng. Struct. Dyn. 39 (13), 1421–1442.
Huang, Y.-N., Whittaker, A.S., Luco, N., 2011. A probabilistic seismic risk assessment procedure for nuclear power plants: (i) methodology. Nucl. Eng. Des. 241 (9), 3996–4003.
Huang, Y.-N., Whittaker, A.S., Luco, N., 2011. A probabilistic seismic risk assessment procedure for nuclear power plants: (ii) application. Nucl. Eng. Des. 241 (9), 3985–3995.
IAEA, 2009. Evaluation of Seismic Safety for Existing Nuclear Installations. Technical Report NS-G-2.13. International Atomic Energy Agency, Vienna.
Jalayer, F., 2003. Direct Probabilistic Seismic Analysis: Implementing Non-linear Dynamic Assessments. Stanford University, Palo-Alto, CA (Ph.D. thesis).
Jalayer, F., De Risi, R., Manfredi, G., 2015. Bayesian cloud analysis: efficient structural fragility assessment using linear regression. Bull. Earthq. Eng. 13 (4), 1183–1203.
Jayaram, N., Lin, T., Baker, J., 2011. A computationally efficient ground-motion selection algorithm for matching a target response spectrum mean and variance. Earthquake Spectra 27, 797–815.
Kabanda, J., Kwon, O.-S., Kwon, G., 2015. Time and frequency domain analyses of the hualien large-scale seismic test. Nucl. Eng. Des. 295, 261–275.
Kemeny, J.G., 1979. Report of the president's commission on the accident at three mile island. The need for change: The Legacy of TMI.
Kennedy, R., Ravindra, M., 1984. Seismic fragilities for nuclear power plant risk studies. Nucl. Eng. Des. 79 (1), 47–68.
Kim, J.H., Choi, I.-K., Park, J.-H., 2011. Uncertainty analysis of system fragility for seismic safety evaluation of NPP. Nucl. Eng. Des. 241 (7), 2570–2579.
Klügel, J.-U., 2005. Problems in the application of the SSHAC probability method for assessing earthquake hazards at swiss nuclear power plants. Eng. Geol. 78 (3-4), 285–307.
Kumar, M., Whittaker, A.S., Constantinou, M.C., 2017. Extreme earthquake response of nuclear power plants isolated using sliding bearings. Nucl. Eng. Des. 316, 9–25.
Kumar, M., Whittaker, A.S., Kennedy, R.P., Johnson, J.J., Kammerer, A., 2017. Seismic probabilistic risk assessment for seismically isolated safety-related nuclear facilities. Nucl. Eng. Des. 313, 386–400.
Kumar, S., Raychowdhury, P., Gundlapalli, P., 2015. Response analysis of a nuclear containment structure with nonlinear soil-structure interaction under bi-directional ground motion. Int. J. Adv. Struct. Eng.(IJASE) 7 (2), 211–221.
Lamea, M., Mirzabozorg, H., 2016. Alkali aggregate reaction effects on an arch dam behaviour including simulation of construction stages and contraction joints. Struct. Eng. Int. 26 (1), 37–44.
Lapajne, J., Fajfar, P., 1997. Seismic hazard reassessment of an existing NPP in slovenia. Nucl. Eng. Des. 175 (3), 215–226.
Larive, C., 1998. Apports Combinés de l'Experimentation et de la Modélisation à la Comprehension del'Alcali-Réaction et de ses Effets Mécaniques. Ecole Normale des Ponts et Chaussées, Paris Technical report (in French).
Le Duy, T.D., Vasseur, D., Serdet, E., 2016. Probabilistic safety assessment of twin-unit nuclear sites: methodological elements. Reliab. Eng. Syst. Saf. 145, 250–261.
Lee, H., Ou, Y.-C., Roh, H., Lee, J.S., 2015. Simplified model and seismic response of integrated nuclear containment system based on frequency adaptive lumped-mass stick modeling approach. KSCE J. Civil Eng. 19 (6), 1757–1766.
Léger, P., Côte, P., Tinawi, R., 1996. Finite element analysis of concrete swelling due to alkali-aggregate reactions in dams. Comput. Struct. 60 (4), 601–611.
Li, K., Coussy, O., 2002. Concrete ASR degradation: from material modeling to structure assessment. Concr. Sci. Eng. 4 (13), 35–46.
Liaudat, J., Carol, I., López, C.M., Saouma, V.E., 2018. ASR expansions in concrete under triaxial confinement. Cem. Concr. Compos. 86, 160–170.
Lysmer, J., Kuhlemeyer, R., 1969. Finite element model for infinite media. ASCE. J. Eng. Mech. 95 (EM 4), 859–877.
Mackie, K., Stojadinovic, B., 2005. Comparison of incremental dynamic, cloud, and stripe methods for computing probabilistic seismic demand models. In: Proceedings of the

2005 Structures Congress and the 2005 Forensic Engineering Symposium, New York, NY.
Mashayekhi, M., Estekanchi, H.E., Vafai, H., Mirfarhadi, S.A., 2018. Development of hysteretic energy compatible endurance time excitations and its application. Eng. Struct. 177, 753–769.
Medel-Vera, C., Ji, T., 2016. Seismic probabilistic risk analysis based on stochastic simulation of accelerograms for nuclear power plants in the uk. Prog. Nucl. Energy 91, 373–388.
Medel-Vera, C., Ji, T., 2016. Seismic risk control of nuclear power plants using seismic protection systems in stable continental regions: the uk case. Nucl. Eng. Des. 307, 377–391.
Miller, C., Cubbage, A., Dorman, D., Grobe, J., Holahan, G., Sanfilippo, N., 2011. Recommendations for Enhancing Reactor Safety in the 21st Century; The Near-Term Task Force Review of Insights from the Fukushima Dai-Ichi Accident.
ML112241029, N., 2011. Concrete degradation by alkali-silica reaction. Online (accessed 2018-07-03).
Mohanty, W.K., Verma, A.K., 2013. Probabilistic seismic hazard analysis for Kakrapar atomic power station, Gujarat, India. Natural Hazards 69 (1), 919–952.
Nakajima, M., Choi, I.-K., Ohtori, Y., Choun, Y.-S., 2007. Evaluation of seismic hazard curves and scenario earthquakes for korean sites based on probabilistic seismic hazard analysis. Nucl. Eng. Des. 237 (3), 277–288.
Nakamura, N., 2008. Seismic response analysis of deeply embedded nuclear reactor buildings considering frequency-dependent soil impedance in time domain. Nucl. Eng. Des. 238 (7), 1845–1854.
Nakamura, N., Akita, S., Suzuki, T., Koba, M., Nakamura, S., Nakano, T., 2010. Study of ultimate seismic response and fragility evaluation of nuclear power building using nonlinear three-dimensional finite element model. Nucl. Eng. Des. 240 (1), 166–180.
Nakamura, S., Nakamura, N., Suzuki, T., Inoda, K., Kosaka, K., 2012. Study on the influence of irregular ground and adjacent building on the seismic response of nuclear power plant building. In: Proc. 15 the World Conference of Earthquake Engineering.
Nour, A., Cherfaoui, A., Gocevski, V., Léger, P., 2016. Probabilistic seismic safety assessment of a candu 6 nuclear power plant including ambient vibration tests: case study. Nucl. Eng. Des. 304, 125–138.
Individual Plant Examination of External Events (IPEEE) for Severe Accident Vulnerabilities – 10CFR 50.54(f). Technical report, Nuclear Regulatory Commission. Generic Letter No. 88–20, Supplement 4.
NRC, 2015. U.S. Nuclear Regulatory Commission Regulations: Title 10, Code of Federal Regulations; PART 54 Requirements for renewal of operating licenses for nuclear power plants.
NRC Office of Public Affairs, 2018. Reactor license renewal. Online (accessed 2018-07-09).
NUREG 1150, 1990. Severe Accident Risks: An Assessment for Five U.S. Nuclear Power Plants.
NUREG-2201, 2016. Probabilistic Risk Assessment and Regulatory Decision making: Some Frequently Asked Questions. Nuclear Regulatory Commission, Washington, DC: US.
NUREG/CR-6706, 2001. NUREG/CR-6706: Capacity of Steel and Concrete Containment Vessels With Corrosion Damage.
Omikrine, M., Kchakech, B., Lavaud, S., Godart, B., 2016. A new model for the analysis of the structural/mechanical performance of concrete structures affected by def-case study of an existing viaduct. Struct. Concr.
Pan, J., Feng, Y., Jin, F., Zhang, C., 2013. Numerical prediction of swelling in concrete arch dams affected by alkaliaggregate reaction. Eur. J. Environ. Civil Eng. 17 (4), 231–247.
Pan, J., Jin, F., Xu, Y., Zhang, C., Feng, Y., 2012. Seismic damage-cracking analysis of concrete dams affected by alkali-aggregate reaction. In: Proceedings of the 15th World Conference in Earthquake Engineering, Lisbona, Portugal.
Pan, J., Xu, Y., Jin, F., Zhang, C., 2014. A unified approach for long-term behavior and seismic response of AAR-affected concrete dams. Soil Dyn. Earthquake Eng. 63, 193–202.
Park, J.-B., Park, N.-C., Lee, S.-J., Park, Y.-P., Choi, Y., 2017. Seismic analysis of the apr1400 nuclear reactor system using a verified beam element model. Nucl. Eng. Des. 313, 108–117.
PEER, 2017. PEER Ground Motion Database. (accessed: 2018–07-16).
Perotti, F., Domaneschi, M., De Grandis, S., 2013. The numerical computation of seismic fragility of base-isolated nuclear power plants buildings. Nucl. Eng. Des. 262, 189–200.
Pian, J., Feng, Y., Wang, J., Sun, C., Zhang, C., Owen, D., 2012. Modeling of alkali-silica reaction in concrete: a review. Front. Struct. Civ. Eng. 6 (1), 1–18.
Porter, K., 2017. When addressing epistemic uncertainty in a lognormal fragility function, how should one adjust the median? In: Proceedings of the 16th World Conference on Earthquake Engineering, Santiago, Chile.
Porter, K., Kennedy, R., Bachman, R., 2007. Creating fragility functions for performance-based earthquake engineering. Earthquake Spectra 23, 471–489.
Progress Energy, 2009. Crystal river unit #3 containment delamination update (accessed: 2018–07-16).
RA-S, ASME, 2008. Standard for Level 1/Large Early Release Frequency Probabilistic Risk Assessment for Nuclear Power Plant Applications. American Society of Mechanical Engineers.
Renault, P., 2014. Approach and challenges for the seismic hazard assessment of nuclear power plants: the swiss experience. Bollettino di Geofisica Teorica ed Applicata 55 (1).
Rezaeian, S., Der Kiureghian, A., 2008. A stochastic ground motion model with separable temporal and spectral nonstationarities. Earthquake Eng. Struct. Dyn. 37 (13), 1565–1584.
Rezaeian, S., Der Kiureghian, A., 2010. Simulation of synthetic ground motions for specified earthquake and site characteristics. Earthquake Eng. Struct. Dyn. 39 (10), 1155–1180.
Rodriguez, J., Lacoma Aller, L., Martinez Cutillas, F., Marti Rodriguez, J., 2011. Contribution to theme a of the benchmark workshop: effect of concrete swelling on the equilibrium and displacements of an arch dam. In: Proceedings of the XI ICOLD Benchmark Workshop on Numerical Analysis of Dams, Valencia, Spain.
Rogovin, M., Grampton, G., 1980. the Nuclear Regulatory Commission (NRC) Special Inquiry Group (1980), Three Mile Island: A report to the Commission and the public (NUREG/CR-1250, 1). US Nuclear Regulatory Commission, Washington, DC.
Ryu, J.-S., Seo, C.-G., Kim, J.-M., Yun, C.-B., 2010. Seismic response analysis of soil-structure interactive system using a coupled three-dimensional FE-IE method. Nucl. Eng. Des. 240 (8), 1949–1966.
Saouma, V., 2017. Effect of AAR on Shear Strength Panels. Technical report, University of Colorado, Boulder. Final Report to NRC, Grant No. NRC-HQ-60-14-G-0010, Task 1-C.
Saouma, V., 2017. Probabilistic Based Nonlinear Seismic Analysis of Nuclear Containment Vessel Structures with AAR. Technical report, University of Colorado, Boulder. Final Report to NRC, Grant No. NRC-HQ-60-14-G-0010, Task 3-B.
Saouma, V., Hariri-Ardebili, M., 2016. Merlin validation & application of aar problems per rilem tc 259-isr guidelines. Technical report. University of Colorado, Boulder Draft Internal Report, 135 pages.
Saouma, V., Hariri-Ardebili, M., Le Pape, Y., Balaji, R., 2016. Effect of alkali-silica reaction on the shear strength of reinforced concrete structural members. A numerical and statistical study. Nucl. Eng. Des. 310, 295–310.
Saouma, V., Miura, F., Lebon, G., Yagome, Y., 2011. A simplified 3d model for rock-structure interaction with radiation damping and free field input. Bull. Earthq. Eng. 9, 1387–1402.
Saouma, V., Perotti, L., 2006. Constitutive model for alkali aggregate reactions. ACI Mater. J. 103 (3), 194–202.
Saouma, V., Perotti, L., Shimpo, T., 2007. Stress analysis of concrete structures subjected to alkali-aggregate reactions. ACI Mater. J. 104 (5), 532–541.
Saouma, V., Sellier, A., Multon, S., Le Pape, Y., Hariri-Ardebili, M., 2017. Benchmark Problems for AAR FEA Code Validation.
Saouma, V., Červenka, J., Reich, R., 2010. Merlin finite element user's manual.
Saouma, V., 2014. Numerical Modeling of AAR. CRC Press 324 pages.
Saxena, N., Paul, D., Kumar, R., 2011. Effects of slip and separation on seismic SSI response of nuclear reactor building. Nucl. Eng. Des. 241 (1), 12–17.
Schroer, S., Modarres, M., 2013. An event classification schema for evaluating site risk in a multi-unit nuclear power plant probabilistic risk assessment. Reliab. Eng. Syst. Saf. 117, 40–51.
Sellier, A., Bourdarot, E., Multon, S., Cyr, M., Grimal, E., 2009. Combination of structural monitoring and laboratory tests for assessment of alkali aggregate reaction swelling: application to gate structure dam. ACI Mater. J. 281–290.
Sextos, A., Manolis, G., Athanasiou, A., Ioannidis, N., 2017. Seismically induced uplift effects on nuclear power plants. Part 1: Containment building rocking spectra. Nucl. Eng. Des. 318, 276–287.
Takatura, T., Ishikawa, T., Matsumoto, N., Mitsuki, S., Takiguchi, K., Masuda, Y., 2005. Investigation of the expanded value of turbine generator foundation affected by alkali-silica reaction. In: 18th International Conference on Structural Mechanics in Reactor Technology (SMIRT 18), Beijing, China. SMIRT18-H03-7, pp. 2061–2068.
USGS, 2017. Unified Hazard Tool (accessed: 2018-07-16).
USGS 2003, 2003. PSHA Interactive Deaggregation Tool, U.S. Geological Survey.
Vamvatsikos, D., Cornell, C., 2002. Incremental dynamic analysis. Earthquake Eng. Struct. Dynam. 31, 491–514.
Vamvatsikos, D., Fragiadakis, M., 2010. Incremental dynamic analysis for estimating seismic performance sensitivity and uncertainty. Earthquake Eng. Struct. Dynam. 39, 141–163.
Verma, A.K., Ajit, S., Muruva, H.P., 2015. Seismic PSA of nuclear power plants. In: Risk Management of Non-Renewable Energy Systems. Springer, pp. 177–254.
Wald, D.J., Allen, T.I., 2007. Topographic slope as a proxy for seismic site conditions and amplification. Bull. Seismol. Soc. Am. 97 (5), 1379–1395.
WASH-1400, 1975. An Assessment of Accident Risks in us Commercial Nuclear Power Plants. NTIS.
Wilson, E., 2014. The Use of the Response Spectrum Method in Earthquake Engineering must be Terminated (accessed: 2018-10-12).
Wojslaw, K., Wisniewski, M., 2014. Nonlinear and Time Dependent Analysis of a Concrete Bridge Suffering From Alkali-silica Reaction: A Case Study of The Elgeseter Bridge in Trondheim. Norwegian University of Science and Technology, Institutt for konstruksjonsteknikk (Master's thesis).
Xu, J., Miller, C., Costantino, C., Hofmayer, C., Graves, H., 2005. Assessment of seismic analysis methodologies for deeply embedded NPP structures. Brookhaven National Laboratory (US) Technical report.
Yamamoto, Y., Baker, J.W., 2013. Stochastic model for earthquake ground motion using wavelet packets. Bull. Seismol. Soc. Am. 103 (6), 3044–3056.
Zentner, I., Humbert, N., Ravet, S., Viallet, E., 2011. Numerical methods for seismic fragility analysis of structures and components in nuclear industry-application to a reactor coolant system. Georisk 5 (2), 99–109.
Zhao, C., Chen, J., 2013. Numerical simulation and investigation of the base isolated NPPC building under three-directional seismic loading. Nucl. Eng. Des. 265, 484–496.